



## Attestation de contrat doctoral

Je soussigné Grégoire CASALIS, Directeur de la Recherche et des Ressources Pédagogiques de l'ISAESUPAERO, atteste que, sous réserve de l'avis favorable de l'école doctorale Systèmes et de l'autorisation d'inscription, Sébastien VELUT bénéficiera d'un contrat doctoral de 36 mois avec l'ISAE-SUPAERO à compter de la rentrée 2023/2024 pour le projet de thèse intitulé «*Understanding and addressing within-user variability in Brain-Computer Interfaces*», co-dirigé par Frédéric DEHAIS (ISAE-SUPAERO) et Sylvain Chevallier (LISN). Sa rémunération sera de 2362€ brut/mois.

Signé électroniquement  
le 25/07/2023 par Gregoire CASALIS

  
ISAE SUPAERO  
Grégoire Casalis  
Directeur de la Recherche  
et des Ressources Pédagogiques  
Grégoire CASALIS

Directeur de la Recherche et des Ressources Pédagogiques



**ISAE SUPAERO - Institut Supérieur de l'Aéronautique et de l'Espace**

10, avenue Edouard-Belin - BP 54032 - 31055 Toulouse CEDEX 4 - FRANCE  
Tél : 33 (0)5 61 33 80 80 - Télécopie : 33 (0)5 61 33 83 30 - Site internet : [www.isae-supero.fr](http://www.isae-supero.fr)

# Sébastien Velut

Étudiant à l'ISAE SUPAERO en dernière année

Je suis ingénieur de l'ISAE SUPAERO, je suis motivé et travailleur. Je suis depuis mon dernier stage très intéressé par la neuroscience et l'IA. Je voudrais donc effectuer une thèse dans le monde de la neuroIA.

sebvelut28@gmail.com

0618358529

137 rue des Meuniers, 92220, Bagneux

## Études

### Diplôme d'ingénieur en aérospatial (Msc)

ISAE-SUPAERO, Toulouse

09/2018 – présent

- Mathématiques appliquées
- Physique
- Machine Learning
- Informatique

### Classe préparatoire MP\* (Maths, physique)

Lycée Carnot, Dijon

09/2016 – 07/2018

- Cours intensifs pour se préparer à l'examen d'entrée de SUPAERO.
- 40 h par semaine de cours théoriques avec option science de l'ingénieur.

## Compétences

- Python C/C++ Java Unity LateX  
Travail en équipe Gestion du stress  
Organisation Persévérance Matlab

## Diplômes

- Permis B (04/2018)
- Baccalauréat scientifique option SI mention très bien (07/2016)
- Brevet d'initiation en aéronautique (06/2014)
- Diplôme du Bachelor de l'ISAE SUPAERO en sciences de l'ingénieur

## Langues

- Anglais C1 (TOEFL ITP 590 points)
- Allemand B2
- Japonais A1

## Activités

- Football Squash Basketball  
Observation spatiale en télescope

## Expériences professionnelles

### Data-Manager

Institut Pasteur

10/10/2022-10/08/2023

- Créer et gérer des bases de données dans un projet européen.
- Accompagner les cliniciens et chercheurs dans les bonnes mœurs lors des rentrées de données

### Stage de fin d'étude : Reconnaître les émotions par une caméra infrarouge

ISAE SUPAERO

01/03/2021-02/07/2021

- Développer un programme lisant une vidéo infrarouge et donnant la température du visage au cours du temps.
- Analyser des données et mettre en relation avec d'autres données physiologiques.

### Stage développement d'une interface cerveau-machine (ICM)

ISAE SUPAERO

01/03/2021-02/07/2021

- Développer des applications en C pour des études pour améliorer les performances de l'ICM
- Développer une application en Unity avec le SDK Nextmind pour une expérience EEG en cockpit d'avion

### Stage en recherche sur l'analyse des performances scientifiques de l'instrument X-IFU

IRAP

15/09/2020-19/02/2021

- Étudier les performances de X-IFU pour l'observation d'objets brillants et compacts
- Simuler, étudier et analyser des spectres venant de X-IFU

### Stage développement d'un outil de simulation de duel

MBDA

16/03/2020-21/08/2020

- Étudier et améliorer les capacités d'un missile antibalistique à ralentir et accélérer
- Simuler des duels et mettre en forme les résultats obtenus

### Responsable des sports

Association sportive de l'ISAE SUPAERO

01/2019 – 12/2019

- Superviser les relations entre l'AS ISAE SUPAERO et PSA31 (l'entreprise mettant à disposition les entraîneurs)
- S'occuper des validations de remboursements de certains sports

## Proposition de sujet de de Thèse - 2023 - Vague 3

**Équipe de recherche** 1 Decisio/DCAS .....

**Équipe de recherche** 2 (le cas échéant) .....

### Directeur de thèse

Nom : Dehais

Prénom : Frédéric

Courriel : [frederic.dehais@isae-sup Aero.fr](mailto:frederic.dehais@isae-sup Aero.fr)

HDR  Oui, délivrée le...29 juin 2022..... par l'Université Paul

Sabatier.....

Non

### Co-Directeur de thèse

Nom : Chevallier

Prénom : Sylvain

Courriel : [sylvain.chevallier@universite-paris-saclay.fr](mailto:sylvain.chevallier@universite-paris-saclay.fr)

HDR  Oui, délivrée le 4 décembre 2019

par l'Université de Versailles St Quentin

Non

### 1. Sujet de thèse (limité à 3 pages pleines sans la bibliographie)

Comprendre et traiter la variabilité intra-utilisateur dans les interfaces cerveau-ordinateur

Les interfaces cerveau-machine (ICM) sont des dispositifs qui offrent une voie de communication directe entre le système nerveux et une machine (Clerc et al, 2016). Les ICM peuvent s'appliquer à la prévention et à la résolution de problèmes engendrés par des troubles cognitifs et moteurs (interface passive) ou optimiser le couplage d'un opérateur (ex : pilote) avec les systèmes qu'il supervise (ex : pilote automatique). La mise en œuvre de telle ICM requiert en premier lieu l'utilisation de technologie de mesures cérébrales. Ces dernières années ont vu l'essor de nombreuses méthodologies en électro-encéphalographie (EEG) non-invasives permettant un décodage en « temps réel » de la dynamique des réponses cérébrales. En parallèle, nous assistons à une popularisation de l'EEG avec l'émergence de systèmes portatifs grand public, grâce à la miniaturisation des composants et l'augmentation de la puissance des calculateurs embarqués. Dans ce contexte, il existe deux approches principales dans le développement des ICM (Clerc et al, 2016; Zander, & Kothe, 2011).

Une première approche cherche à mettre en œuvre des ICM dites actives/réactives qui permettent à un utilisateur de contrôler volontairement un système (ex : chaise roulante, curseur d'une souris) à l'aide de ses ondes cérébrales. Dans le cadre des ICM actives, l'utilisateur doit s'entraîner à produire consciemment des signaux cérébraux « simples » et « clairs », par exemple en se relaxant (ondes alpha) ou en réalisant de l'imagerie motrice mentale (par ex : imaginer un mouvement de la main droite) afin d'y associer une commande (ex : déplacer à droite un curseur). La machine apprend en premier lieu à reconnaître les signaux d'intérêts de manière supervisée lors d'une phase de calibration. Or cette phase de calibration est généralement longue (~15/20 minutes et demande une forte concentration pour un nombre de commandes très limité (~4). De plus elle doit être répétée pour chaque nouvelle utilisation de l'ICM. Une approche alternative consiste à développer des ICM « réactives » où cette fois les signaux cérébraux d'intérêts sont produits en réaction à un stimuli externe (visuel, sonore, tactile) Par exemple, la focalisation du sujet sur un stimulus visuel flashant à une fréquence précise entraîne une augmentation de son activité cérébrale, mesurée avec l'EEG, dans cette même bande de fréquence (Allison et al, 2010). Ainsi en plaçant des stimulus visuels avec des fréquences différentes sur des emplacements distincts d'un écran, on peut y associer des commandes pour diriger un robot dans l'espace. Les ICM réactives basées sur des stimulus

visuels présentent des performances de classification élevées (Chevallier et al, 2021; Nakanishi et al, 2018; Nagel et al, 2019). La haute discriminabilité des réponses neuronales permet de concevoir des interfaces avec de nombreuses commandes, par exemple un clavier de 40 classes (Nakanishi et al, 2018). Néanmoins, les ICM réactives présentent de nombreux inconvénients pour les utilisateurs finaux. Par exemple, la calibration reste longue et sa durée dépend directement du nombre de commandes du système. Enfin, la limitation principale est que la plupart des ICM réactives sont des systèmes synchrones, ce qui signifie le système a besoin de connaître l'instant exact où le sujet commence à regarder le stimulus. En pratique, le système a un rythme figé qui alterne entre stimuli et pause afin de contraindre le rythme pour l'utilisateur, ce qui offre un sentiment de contrôle moindre. Pour finir, le scintillement des stimuli induit une fatigue oculaire de l'utilisateur et un risque d'épisodes épileptiques pour les sujets photosensibles.

Une deuxième approche cherche à développer des ICMs passives, dont le but n'est alors plus de contrôler volontairement un effecteur mais de décoder l'état mental du sujet pour enrichir l'interaction homme-machine de manière implicite (Zander, & Kothe, 2011). Les états mentaux habituellement considérés sont le niveau de charge mentale, la fatigue ou le niveau d'attention (Gateau et al., 2018 ; Dehais et al., 2018, 2019) ou la fatigue. Cette estimation permet en retour d'adapter dynamiquement l'interface pour maintenir une performance optimale (Aricò et al., 2017). Généralement, l'estimation des états mentaux est réalisée par des analyses temporelles ou fréquentielles du signal électrophysiologique (Borghini et al, 2014; Brouwer et al, 2013).). Tout comme pour les méthodes actives/réactives il faut au préalable collecter des données pour calibrer les algorithmes ce qui nécessite l'induction d'états mentaux spécifiques (par exemple, différents niveaux de stress ou d'attention) de manière répétitive. C'est bien sur problématique si la situation est particulièrement désagréable pour le sujet et il est particulièrement difficile de créer de telles situations de manière répétée et réaliste en laboratoire. Enfin, cette phase d'apprentissage doit être réalisée avant chaque utilisation, ce qui limite son intérêt dans les situations de la vie courante.

L'ensemble de ces travaux montrent qu'en dépit de leur intérêt dans de nombreux domaines, les ICM restent confinés au cadre du laboratoire principalement pour des problèmes de performance et de confort (calibration longue, flash visuels intrusifs, dispositifs non asynchrones). Aussi dans le cadre de cette thèse nous proposons une nouvelle approche pour développer une ICM robuste et transparente et duale dans son utilisation. Par robuste et transparente dans son utilisation, nous sous-entendons que l'ICM sera asynchrone (i.e. déclenchée et contrôlée par l'utilisateur), aura des temps de calibration extrêmement rapide (environ 1 à 2 minutes) avec des performances de justesse de prédiction >90%. La conception des « flashes visuels » sera améliorée pour les rendre quasi transparents et confortables tout en permettant leur décodage par les algorithmes d'apprentissage machine. Par duale, nous souhaitons que l'ICM soit à la fois réactive et passive pour permettre une interaction bi-directionnelle. En effet, les ICM réactive et passives ont jusqu'à présent été utilisées séparément, alors que de nombreuses tâches de la vie quotidienne impliquent conjointement des interactions volontaires avec une interface utilisateur et la surveillance de l'état de la machine. En outre, le même dispositif (par exemple, l'EEG) pourrait être utilisé pour recueillir des données cérébrales et alimenter différents algorithmes chargés de contrôler une interface et de déduire l'état mental de l'utilisateur. Une telle approche ouvrirait la voie à la conception d'un nouveau concept de technologie neuroadaptative, à savoir une ICM Duale.

Une première étape pour mettre en œuvre une telle ICM transparente associée à une courte calibration sera amené de considérer les stimulations nommées « code-VEP ». Au lieu de flasher de manière périodique, l'affichage du stimulus suit une séquence binaire pseudo-aléatoire apériodique. Des études utilisant ce paradigme ont pu obtenir des performances très convaincantes (Thielen et al, 2015; Naegel et al, 2019; Turi et al, 2020) associées à des calibrations réduites, en comparaison des stimuli périodiques plus classiques. Par ailleurs, une étude est en cours à l'ISAE-SUPAERO a obtenu des résultats préliminaires allant également dans ce sens. Il s'agira donc de capitaliser sur ces bons résultats et poursuivre dans l'optique de réduction de calibration.

Il sera ensuite nécessaire de développer de nouveaux algorithmes de classification automatiques. Pour cela, une piste intéressante pour le candidat sera d'utiliser de réseaux de neurones convolutifs. Ce sont ces mêmes réseaux qui ont donné lieu à une révolution dans le domaine de la vision par ordinateur en 2012 puis du traitement du langage naturel quelques années plus tard. Bien qu'il existe déjà quelques démonstrations convaincantes de l'utilisation de tels réseaux pour la classification de signaux cérébraux (Nagel et al, 2019; Vernont et al, 2016; Banville et al, 2021), beaucoup reste encore à développer en comparaison des autres domaines de l'apprentissage automatiques. Ces réseaux nous semblent des candidats prometteurs car ce sont ceux les plus à même de modéliser des relations courtes distances. En effet, les réponses cérébrales à un stimuli visuel sont de l'ordre de 250ms ce qui correspond à 125 points pour un système EEG possédant une fréquence d'échantillonnage de 500Hz. Par ailleurs et c'est un des principaux challenges, il faudra associer à ces réseaux de neurones de nouveaux processus de décision asynchrones, opérant sur des durées flexibles afin de dépasser les limites et la rigidité d'un point de vue utilisateur des interfaces synchrones existantes. Enfin, ces réseaux de neurones convolutifs offrent également des possibilités bien établies pour transférer l'apprentissage depuis un problème particulier

(un sujet dans notre cas) vers un autre sujet (un autre sujet) : transfert learning, zero shot learning, self-supervised learning. Ces transferts d'apprentissage pourraient très probablement permettre de réduire la calibration en utilisant des données d'autres sujets ou tâches en complément (Wei et al, 2022). Il n'existe pour l'heure pas de base de données publiques EEG pour le paradigme du code-VEP. Dans une démarche de science ouverte et collaborative, nous proposerons de collecter et diffuser une telle base de données.

Le dernier objectif de ce projet de thèse consistera à développer de nouveaux stimulus visuels plus confortables, avec une meilleure expérience utilisateur. Actuellement les ICM réactives utilisant le code-VEP pour la stimulation font clignoter de simples rectangles unis, avec un contraste maximal. Des travaux en cours à l'ISAE-SUPAERO ont montré qu'il est possible de réduire le contraste de la stimulation pour les rendre perceptuellement presque invisibles tout en gardant des performances satisfaisantes (Ladouce et al, 2022). Nous pensons qu'il reste beaucoup à explorer, notamment au travers des textures, couleurs et formes de stimulus. De manière avantageuse cette approche pourrait être adaptée aux ICMs passives afin de détecter le niveau d'attention et de vigilance des utilisateurs sur différentes zones d'une interface. En plaçant ces stimuli transparents à l'arrière-plan de différentes régions d'intérêt, on pourra mesurer l'intensité de la réponse du cerveau et en déduire le niveau d'attention alloué à ces zones spécifiques. Il serait attendu par exemple qu'un utilisateur engagé et attentif aura des réponses plus intenses alors qu'un utilisateur hypovigilant aura des réponses cérébrales plus faibles. En conséquent nous pourrons utiliser ces mesures pour adapter l'interaction (ex : transfert d'autorité vers le pilote automatique en cas d'hypovigilance) entre l'humain et les systèmes qu'ils contrôlent. L'intérêt de cette approche sera d'utiliser la même calibration pour l'ICM réactive et l'ICM passive et permettre le développement d'une véritable ICM duale.

Concrètement, le plan de travail sera le suivant

#### Première année de thèse

État de l'art s'appuyant en 1er lieu sur les travaux en stage de clôture du candidat M. Velut, en cours et les connaissances accumulées au cours des 2 dernières années par l'équipe de l'ISAE-SUPAERO

Constitution d'une base de données (sur le modèle de celle en SSVEP de Nakashima) et publication en ligne, au travers la plateforme MOABB : design expérimental et développement de l'interface, collecte de données avec une vingtaine de sujets, traitement des données et développement d'une méthode d'analyse automatique et statique.

#### Deuxième année de thèse

Développement de nouveaux algorithmes, procédures d'entraînement et processus de décision asynchrone (séquençage en 2 étapes pour détecter dans une première étape si l'utilisateur regarde n'importe quel stimulus puis l'identification de celui-ci).

Développement de stimuli maximisant l'expérience utilisateur tout en conservant un compromis avec la performance.

Réalisation d'expérimentations avec une vingtaine de sujets.

#### Troisième année de thèse :

Transfert et adaptation de la chaîne de traitement pour l'utilisation avec des casques EEG à électrodes sèches (i.e. sans gel) pour améliorer le confort des utilisateurs. Expérimentation avec une dizaine de sujets

Rédactions du manuscrit de thèse

## Bibliographie

Arico, P., Borghini, G., Di Flumeri, G., Sciaraffa, N., Colosimo, A., & Babiloni, F. (2017). Passive BCI in operational environments: insights, recent advances, and future trends. *IEEE Transactions on Biomedical Engineering*, 64(7), 1431-1436.

Banville et al (2021) Uncovering the structure of clinical EEG signals with self-supervised learning. *Journal of Neural Engineering*.

Borghini, G., Astolfi, L., Vecchiato, G., Mattia, D., & Babiloni, F. (2014). Measuring neurophysiological signals in aircraft pilots and car drivers for the assessment of mental workload, fatigue and drowsiness. *Neuroscience & Biobehavioral Reviews*, 44, 58-75.

Brouwer, A. M., Hogervorst, M. A., Van Erp, J. B., Heffelaar, T., Zimmerman, P. H., & Oostenveld, R. (2012). Estimating workload using EEG spectral power and ERPs in the n-back task. *Journal of neural engineering*, 9(4), 045008.

Chevallier, S., Kalunga, E. K., Barthélémy, Q., and Monacelli, E. (2021). Review of riemannian distances and divergences, applied to SSVEP-based BCI. *Neuroinformatics* 19, 93–106.

Clerc, M., L. Bougrain, L., F. Lotte (2016) "Les Interfaces Cerveau-Ordinateur 1 : fondements et méthodes / Les Interfaces Cerveau-Ordinateur 2 : technologie et applications", ISTE-Wiley.

Dehais, F., Dupres, A., Di Flumeri, G., Verdiere, K., Borghini, G., Babiloni, F., & Roy, R. (2018, October). Monitoring pilot's cognitive fatigue with engagement features in simulated and actual flight conditions using an hybrid fNIRS-EEG passive BCI. In 2018 IEEE international conference on systems, man, and cybernetics (SMC) (pp. 544-549). IEEE.

Dehais, F., Duprè, A., Blum, S., Drougard, N., Scannella, S., Roy, R. N., & Lotte, F. (2019). Monitoring pilot's mental workload using ERPs and spectral power with a six-dry-electrode EEG system in real flight conditions. Sensors, 19(6), 1324.

Gateau, T., Ayaz, H., & Dehais, F. (2018). In silico vs. over the clouds: on-the-fly mental state estimation of aircraft pilots, using a functional near infrared spectroscopy based passive-BCI. Frontiers in human neuroscience, 12, 187.

Ladouce, S., Darmet, L., Torre Tresols, J. J., Velut, S., Ferraro, G., & Dehais, F. (2022). Improving user experience of SSVEP BCI through low amplitude depth and high frequency stimuli design. Scientific reports, 12(1), 1-12.

Nagel S, Spüler M (2019). World's fastest brain-computer interface: Combining EEG2Code with deep learning. PLOS ONE 14(9). 2019

Thielen J, van den Broek P, Farquhar J, Desain P (2015) Broad-Band Visually Evoked Potentials: Re(con)volution in Brain-Computer Interfacing. PLOS ONE 10(7).

Turi, Nathalie T.H. Gayraud, Maureen Clerc (2020). Auto-calibration of c-VEP BCI by word prediction.

Vernon J. Lawhern, Amelia J. Solon, Nicholas R. Waytowich, Stephen M. Gordon, Chou P. Hung, and Brent J. Lance (2016). EEGNet: A Compact Convolutional Neural Network for EEG-based Brain-Computer Interfaces. Journal of Neural Engineering.

Wei, X., Faisal, A. A., Grosse-Wentrup, M., Gramfort, A., Chevallier, S., Jayaram, V., ... & Tempczyk, P. (2022). 2021 BEETL Competition: Advancing Transfer Learning for Subject Independence & Heterogenous EEG Data Sets. arXiv preprint arXiv:2202.12950.

Zander, T. O., and Kothe, C. (2011). Towards passive brain-computer interfaces: applying brain-computer interface technology to human-machine systems in general. J. Neural Eng. 8:025005. doi: 10.1088/1741-2560/8/2/025005

## 2. Thèses en cours d'encadrement par le ou les directeur(s) de thèse

(Préciser pour chaque encadrement : le nom du doctorant, l'année de thèse, le sujet, le financement et l'école doctorale, et le cas échéant, date de soutenance de la dernière bourse EDSYS obtenue)

### Frédéric Dehais

- Yannick Migliorni (EDSYS, financement DGAC): manuscrit rendu, soutenance le 14 septembre 2022-
- Patrice Labedan (EDSYS, pas de financement): inscription en 6<sup>ème</sup> année (ingénieur de laboratoire isae en temps partiel sur thèse) – soutenance planifiée pour mai 2022
- Giorgio Angelotti (EDSYS, financement ANITI): dernière année de these (en arrêt maladie pour accident)
- Juan Torre Tresols (AA, financement AA/ISAE), deuxième année de thèse

### Sylvain Chevallier

- Isabelle Hoxha (ED SSMMH, Université Paris-Saclay, financement MESRI), thèse débutée en octobre 2020 (3e année), *Mécanismes neurocognitifs de l'anticipation perceptive dans la prise de décision*.
- Maria-Sayu Yamamoto (ED STIC, Université Paris-Saclay, financement ANR UDOPIA), thèse débutée en avril 2021 (2e année), *Similarity-based classification for EEG by considering the Riemannian geometry*.

## 3. Commentaire, avis motivé, nom, date et signature du (des) responsable(s) de(s) l'équipe(s) de recherche (ou équipe d'accueil doctoral)

(Justifier le choix du sujet et son positionnement au sein de l'équipe)



**ECOLE DOCTORALE SYSTEMES - ED309**

Maison de la Recherche et de la Valorisation

118 route de Narbonne

Tel : (33) (0) 5 6 25 00 66

Email : [edsys@laas.fr](mailto:edsys@laas.fr)

Web : <https://www.adum.fr/as/ed/edsys>

Ce projet de recherche, au carrefour des neurosciences et de l'intelligence artificielle, est au cœur des problématiques des recherches menées dans DECISIO. Il est à la fois fondamental (i.e. développements d'algorithmes avancées de décodage de l'information cérébrale) et appliqué dans la mesure où les retombées les ICM pour des applications de santé (handicap) ou de conduire de système critique (ex : pilotage d'avion). En particulier, ces travaux pourront déboucher à terme sur la mise en œuvre de capteurs et d'algorithmes temps réels embarquables pour prédire la dégradation de la performance des pilotes en condition réelle de vol. Nous espérons tout d'abord pouvoir réaliser un transfert technologique auprès des partenaires industriels (Airbus, Thalès et Dassault aviation). Ensuite ces travaux pourront trouver des applications dans de nombreux domaines liés au BCI tels que le gaming ou la médecine (diagnostique/e-santé) notamment dans le cadre de des partenariats du DCAS avec le service de réhabilitation fonctionnelle du CHU de Toulouse Rangueil.

**4. Visa, nom, date et signature du directeur de l'unité de recherche.**

MINISTÈRE DES ARMÉES

INSTITUT SUPÉRIEUR DE L'AÉRONAUTIQUE ET DE L'ESPACE

DIPLÔME D'INGÉNIEUR ISAE-SUPAERO

GRADE DE MASTER - MASTER'S DEGREE

Le directeur général de l'Institut supérieur de l'aéronautique et de l'espace,  
Vu le code de l'Education et notamment ses articles L613-6, L642-12, D642-1 à D642-10  
Vu le code de la Défense et notamment son article R3411-5,  
Vu l'arrêté du 24 janvier 2018 accréditant l'Institut à délivrer le titre d'ingénieur diplômé de l'Institut supérieur de l'aéronautique et de l'espace,

décerne à **VELUT Sébastien, René, Hubert**

date et lieu de naissance : **28 janvier 1999 à Dijon (21)**,

Institut Supérieur de l'Aéronautique et de l'Espace

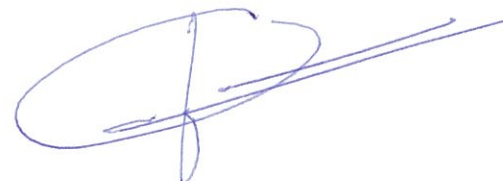
le titre d'ingénieur diplômé de l'Institut supérieur de l'aéronautique et de l'espace, lui conférant le grade de master. Au titre de l'année universitaire 2021/2022

À Toulouse, le 17 novembre 2022

L'ingénieur général de l'armement,

Olivier Lesbre

*Directeur général de l'Institut supérieur  
de l'aéronautique et de l'espace*



**DIPLOME DE BACHELOR**  
**BACHELOR'S DEGREE**

Vu l'article L613-2 du code de l'éducation,  
*In view of article L613-2 of the Education Code.*

Vu la délibération du Conseil d'Administration n° 35/4 du 19 juin 2018 fixant le règlement de scolarité de l'ISAE-SUPAERO,  
*In view of the ISAE-SUPAERO regulations as approved by the Board in decision n°35/4 dated june 19, 2018.*

Vu le Procès-Verbal du jury de passage du 4 juillet 2019.  
*In view of the report of the Board of Examiners dated July 4, 2019,*

Le **DIPLOME DE BACHELOR DE L'ISAE-SUPAERO en sciences de l'ingénieur**  
*The Degree of Bachelor of Engineering Sciences*

est délivré, au titre de l'année universitaire 2018-2019, à M. Sébastien, René, Hubert VELUT, né le 28 janvier 1999 à Dijon (21)  
*has been conferred on Mr. Sébastien René, Hubert VELUT, date of birth: January 28, 1999, place of birth: Dijon (21), for the academic year 2018-2019.*

Le Directeur Général de l'ISAE-SUPAERO,  
*The President of ISAE-SUPAERO*  


Nom : **VELUT**

**Année universitaire : 2021/2022**

Prénom: **SEBASTIEN**

ECTS acquis : 60.0

**CGPA : 4.14**

Enseignements	Notes de sessions		Notes de la promotion			Nb. étudiants	ECTS	Nb. heures	GPA				
	Initiale	Rappel	Moy	Min	Max								
<b>Domaine Neuro-IA</b>													
<b>D - Domaine Neuro-IA</b>													
D-NIA301-Neuroergonomie	18		14.57	12.0	18.0	30	2.5	40h	4.3				
D-NIA302-Expérimentation, Mesures et Interface Cerveau Machine	16		13.33	11.0	17.0	30	2.5	47h	4.0				
D-NIA303-Méthode et outil de l'IA pour la Neuroergonomie	16		15.5	8.0	18.0	30	3	53h	4.0				
<b>Filière Observation de la Terre et Sciences de l'Univers - (OTSU) - S5</b>													
<b>TC - Tronc commun (OTSU)</b>													
F-OTSU301-Physique mesure et capteurs	16		14.95	9.0	19.0	55	2	30h	4.0				
F-OTSU302-Traitement données, signal & images	16		15.3	12.0	18.0	54	3	60h	4.0				
F-OTSU303-Missions scientifiques	15		15.33	13.0	18.0	54	3	40h	4.0				
F-OTSU304-Bases de données et apprentissage profond	18		15.87	10.0	20.0	54	1	25h	4.3				
<b>Parcours Sciences de l'Univers</b>													
F-OTSU310-Harmonisation	13		13.29	11.0	17.0	24	4	50h	3.7				
F-OTSU311-Mécanique céleste avancée	13		14.38	13.0	18.0	24	1	15h	3.7				
F-OTSU312-Gravitation	14		14.8	9.0	20.0	25	1	20h	3.7				
<b>TC - Tronc commun ingénierie et entreprise - S5</b>													
PIE301-Projet ingénierie et entreprise	16		16.26	11.0	19.0	310	5	100h	4.0				
<b>TC - Tronc commun Humanités - S5</b>													
LV1-300-Anglais	16		16.59	0	20.0	316	2	40h	4.0				
<b>Stage de fin d'études - S6</b>													
SFE-Stage de fin d'études	17		17.05	12.0	20.0	298	30	800h	4.3				

A+ = Très bien B+ = Bien C+ = Assez bien D = Insuffisant

Page 1 / 1

Édité à Toulouse le 05/12/2022



Professeur Caroline BERARD  
Directrice des Formations Ingénieurs

Formation d'ingénieur ISAE-SUPAERO (MSc)  
Année 2

Nom : VELUT  
Prénom: SEBASTIEN

Année universitaire : 2020/2021  
ECTS acquis : 24

CGPA : 4.3

Enseignements	Notes de sessions		Notes de la promotion			Nb. étudiants	ECTS	Nb. heures	GPA
	Initiale	Rappel	Moy	Min	Max				
<b>Autres modules S4</b>									
STA93-Stage substitution S4	20		20.0	20.0	20.0	4	24	550h	4.3

A+ = Très bien B+ = Bien C+ = Assez bien D = Insuffisant

Page 1 / 1

Édité à Toulouse le 30/09/2021



Professeur Caroline BERARD  
Directrice des Formations Ingénieurs

ISAE-SUPAERO - Institut Supérieur de l'Aéronautique et de l'Espace

10, avenue Edouard-Belin - BP 54032 - 31055 Toulouse CEDEX 4 - France 33 (0)5 61 33 80 80 - isae@isae.fr - www.isae-supapro.fr

Nom : **VELUT**

**Année universitaire : 2019/2020**

Prénom: **SEBASTIEN**

ECTS acquis : 36.0

**CGPA : 3.99**

<b>Enseignements</b>	<b>Notes de sessions</b>		<b>Notes de la promotion</b>			<b>Nb. étudiants</b>	<b>ECTS</b>	<b>Nb. heures</b>	<b>GPA</b>
	<b>Initiale</b>	<b>Rappel</b>	<b>Moy</b>	<b>Min</b>	<b>Max</b>				
<b>Tronc commun scientifique S3</b>									
TCS3-IN-Informatique	19		14.81	8.0	20.0	296	3.5	50.5h	4.3
TCS3-MA-Mathématiques appliquées	18		13.08	7.0	18.0	297	3	30h	4.3
TCS3-MF-Mécanique et thermodynamique des fluides	16		12.98	6.0	18.0	297	5	65h	4.0
TCS3-MG-Mécanique générale	16		14.38	2.0	19.0	297	3	40.5h	4.0
TCS3-MS-Mécanique des solides déformables	14		13.38	7.0	18.0	300	3.5	48h	3.7
TCS3-PH-Physique	14		13.13	2.5	19.0	295	3	30h	3.7
TCS3-SS-Signaux et systèmes	14		13.48	6.0	19.0	300	5	70h	3.7
<b>Tronc commun Humanités S3</b>									
LV1-200-Anglais	15		15.71	1.0	20.0	298	1.5	20h	4.0
LV2-207-Japonais	19		16.29	12.0	20.0	31	1.5	30h	4.3
AC3-Arts & cultures	19		15.47	8.0	20.0	299	1	17.5h	4.3
PC3-Pratiques corporelles	B+					300	1	27h	3.7
TCH-ICW-Intercultural Workshop	B+					303	1.5	24h	3.7
<b>Tronc commun I&amp;E S3</b>									
IE-201-Ingénierie et Entreprise	18		14.55	3.8	18.0	298	3.5	60h	4.3

A+ = Très bien B+ = Bien C+ = Assez bien D = Insuffisant

Page 1 / 1

Édité à Toulouse le 21/07/2020



Professeur Caroline BERARD  
Directrice des Formations Ingénieurs

Nom : **VELUT**

**Année universitaire : 2018/2019**

Prénom: **SEBASTIEN**

ECTS acquis : 60.0

**CGPA : 3.98**

<b>Enseignements</b>	<b>Notes de sessions</b>		<b>Notes de la promotion</b>			<b>Nb. étudiants</b>	<b>ECTS</b>	<b>Nb. heures</b>	<b>GPA</b>
	<b>Initiale</b>	<b>Rappel</b>	<b>Moy</b>	<b>Min</b>	<b>Max</b>				
<b>Tronc commun scientifique S1</b>									
TCS1-IN-Informatique	18.25		13.45	0	20.0	221	3	40h	4.3
TCS1-MA-Mathématiques appliquées	16.8		13.47	7.4	19.2	216	6	90h	4.0
TCS1-MF-Mécanique et thermodynamique des fluides	17		14.84	9.5	20.0	217	3	45h	4.3
TCS1-MG-Mécanique générale	16		14.72	10.0	18.0	217	4	50h	4.0
TCS1-MS-Mécanique des solides déformables	16.5		13.67	6.0	18.0	215	3	46h	4.0
TCS1-PH-Physique	16.5		13.57	10.0	17.2	218	4	50h	4.0
TCS1-SS-Signaux et systèmes	13.8		13.86	8.7	18.7	217	4	55h	3.7
<b>Autre enseignement S1</b>									
IE-101-Ingénierie et entreprise	17		14.6	6.13	17.0	217	2.5	44h	4.3
<b>Tronc commun Humanités S1</b>									
LV1-100-Anglais	14		15.19	4.5	18.5	216	2.5	40h	3.7
LV2-107-Japonais	18.5		17.34	10.0	19.0	19	1.5	30h	4.3
AC101-Arts & Cultures	14.5		14.92	8.0	20.0	217	1	16h	3.7
PC1-Pratiques corporelles	B+					217	1	25.5h	3.7
<b>Tronc commun humanités S2</b>									
AC102-Arts & Cultures	17		15.76	4.5	20.0	211	1	16h	4.3
LV1-120-Anglais	16		15.55	2.0	20.0	216	1.5	23h	4.0
LV2-127-Japonais	19.5		15.71	0	19.5	19	1.5	16h	4.3
PC2-Pratiques corporelles	A+					214	1	13.5h	4.3
<b>Autres enseignements S2</b>									
IE102-Ingénierie & entreprise	13.3		13.94	10.1	17.1	215	2.5	40h	3.7
PREX-Pratique expérimentale	16		14.9	8.0	19.0	215	2.5	30h	4.0
PIC102-Projets innovation et créativité	12.5			8.13	19.38	211	6	70h	3.3
CONF100-Cycle de conférences	A+					214	0.5	8h	4.3
<b>COURS ELECTIFS</b>									
EAEP-103-Acoustique et ondes de choc	17.2		15.52	12.0	18.9	31	2	30h	4.3
EEOS-101-Relativité générale et cosmologie	17		12.94	6.5	19.5	45	2	30h	4.3
EEOS-102-Physique stellaire et planétologie	18		16.5	10.0	20.0	50	2	30h	4.3
EEOS-103-Ingénierie quantique: calculateurs quantiques, téléportation et	16		12.07	0	17.0	21	2	30h	4.0

A+ = Très bien B+ = Bien C+ = Assez bien D = Insuffisant

Page 1 / 1

Édité à Toulouse le 23/09/2019



Professeur Caroline BERARD  
Directrice des Formations Ingénieurs



Frédéric Dehais (PhD, HDR)  
Professeur à l'ISAE-SUPAERO  
Université de Toulouse

Responsable de l'équipe Neuroergonomie et Facteurs Humains  
Titulaire de la chaire AXA « Neuroergonomie pour la sécurité des Vols » et de la chaire ANITI « Technologie Neuroadaptative »

Toulouse, le 28 juillet 2023

10, Avenue Edouard BELIN  
31055, TOULOUSE FRANCE  
+ 33 5 61 33 83 72  
[frederic.dehais@isae.fr](mailto:frederic.dehais@isae.fr)

Lettre de recommandation pour appuyer la candidature de M. Sébastien Velut à la bourse de l'école doctorale EDSYS.

Monsieur Agnan de Bonneval, directeur d'EDSYS

Je suis responsable pédagogique du domaine NEURO-IA en dernière année de l'ISAE-SUPAERO. Ce domaine créé récemment vise à donner une solide formation pluridisciplinaire dans le domaine des neurosciences et neuro-engineering, du traitement du signal et de l'intelligence artificielle. Monsieur Sébastien Velut a suivi ce cursus dans sa dernière année d'étude dans notre école d'ingénieur. Il a été un étudiant remarquable dans le sens où il s'est montré toujours extrêmement actif dans les différents enseignements et passionné dans les échanges avec les différents enseignant. Il arrive toujours à poser des questions pertinentes et fondamentales même pour des disciplines nouvelles pour lui (ex : neurosciences), démontrant un très fort esprit de réflexion. Il a su démontrer une très forte puissance de travail pour les différents projets qu'il a dû mener en équipe et arriver à obtenir des résultats impressionnantes notamment lors des partiels. A titre d'exemple, il a terminé premier du module de neurosciences avec une moyenne de 18/20. C'est également un étudiant d'une très grande modestie qui est toujours prêt à aider ses camarades.

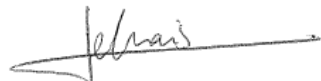
J'avoue ne pas avoir été surpris par la qualité de son travail et son investissement personnel dans notre domaine Neuro-IA. En effet, j'avais eu la chance d'accueillir Sébastien pour un stage de césure de 6 mois au sein de mon laboratoire. Il nous assisté dans le cadre d'un projet de

recherche financé par l'AID et dont le but était de développer des interfaces cerveau machine dites « réactives » pour permettre à un pilote de contrôler « par la pensée » son cockpit sans avoir à utiliser ses mains. Dès son arrivée, Sébastien a su non seulement s'approprier le sujet technique mais s'est intégré parfaitement avec les autres doctorants et post-doctorants impliqués dans le projet en créant une dynamique de travail extrêmement positive. Il nous a amené toute son expérience d'ingénieur pour afficher des stimuli visuels à haute fréquence en C++ et coder une partie temps réel de l'interface cerveau machine. Au-delà de ces apports techniques, Sébastien s'est montré particulièrement intéressé en trouvant des articles de recherche pertinents et en proposant des approches innovantes. J'ai pu apprécier un véritable esprit de chercheur à la fois rigoureux mais aussi très créatif et curieux d'apprendre de nouvelles connaissances utiles et en particulier sur les sujets liés à l'intelligence artificielle. Aussi sa contribution au projet a été essentielle et avons pu publier deux papiers en 2022 où il a été co-auteur dans les revues *Nature Scientific Report* et *Frontiers in Neuroergonomics*. Le projet de thèse sur lequel il candidate s'inscrit dans la pleine continuité des travaux qu'il a mené et qui ont permis de forger ce nouveau concept d'interface cerveau machine transparente et duale. Enfin, pour terminer sur un plan plus personnel, Sébastien est une personne très disponible, extrêmement motivée qui inspire confiance, avec de véritables dispositions pour la pédagogie.

Au vu de ses compétences pluridisciplinaires en ingénierie, neurosciences, et intelligence artificielle et des compétences qu'il a acquise lors de son stage de césure, je ne peux que recommander la candidature de Monsieur Sébastien Velut pour la bourse de l'EDSYS à laquelle il postule. Ses compétences et sa personnalité seront non seulement des atouts pour la réussite de son doctorat mais aussi pour ses projets futurs dans le domaine des neurotechnologies.

Veuillez agréer, Monsieur le directeur de l'EDSYS, l'assurance de ma considération distinguée.

Frédéric Dehais Ph.D.

A handwritten signature in black ink, appearing to read "Dehais".

Defence, Safety & Security  
Kampweg 55  
3769 DE Soesterberg

P.O. Box 23, 3769 ZG Soesterberg

[www.tno.nl](http://www.tno.nl)

Attn. Mr. Bonneval

Date  
4 September 2023

Subject      Recommendation Sébastien Velut

Dear mister Bonneval,

As advisor of Sébastien Velut during his master's internship at TNO Soesterberg, the Netherlands, I was asked to write you a recommendation letter for the PhD position that he aspires. Given my experience with Sébastien, I am more than happy to do so.

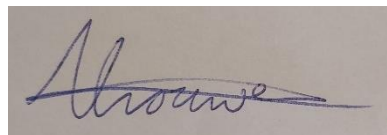
Sébastien has been working in our lab from April up until September 2022. He mainly worked on a study where participants experienced emotions as induced by various paradigms, performed meditation, and were being treated by a practitioner from the alternative medicine circuit. Participants were being recorded using a range of sensors, including EEG, ECG, skin conductance, ultraweak biophoton emission sensors and an infrared camera. Research questions concerned the relation between these different mental states and the recorded signals. Sébastien contributed strongly to organizing and running these complex experiments. Regarding analysis, he focused on the infrared data of the face. We did not have a way yet to analyze these data automatically. Sébastien worked on extracting regions of interest with as little as possible required manual work. This involved searching, implementing and validating face tracking algorithms which do not normally work on infrared images. He searched the literature, extracted sensible variables, and performed statistics. He wrote a very good report, and left us with tools that will greatly facilitate our future studies with infrared face data.

Besides this main project, Sébastien was always happy to support TNO colleagues in other ways. In particular, he joined another project which was on food choice behavior. In this project, visitors were recorded at a three-day festival using skin conductance devices and questionnaires while they are watching a movie clip and tasting food. Sébastien was one of the (friendly and stress resilient) experiment leaders and did excellent work on the audio setup.

The General Terms and Conditions for commissions to TNO, as filed with the Registry of the District Court in the Hague and with the Chamber of Commerce and Industry in The Hague, shall apply to all commissions to TNO. Our General Terms and Conditions are also available on our website [www.tno.nl](http://www.tno.nl). A copy will be sent upon request."

I am very grateful to have had him in our team. Sébastien is strongly motivated, can work independently while also being a team player, he learns quickly, shows initiative and is a responsible and reliable person. Organizing an internship in the Netherlands, with all the social and logistic challenges that come with that, is one of the examples showing his endurance and enthusiasm to try new things. He is strong intellectually, technically and socially. I am absolutely convinced he will be an excellent and successful PhD-student. If you have any specific questions, do not hesitate to contact me.

Sincerely,

A handwritten signature in blue ink, appearing to read "Anne-Marie Brouwer".

Prof. Dr. Anne-Marie Brouwer

# Sébastien Velut

## Thèse : Comprendre et aborder la variabilité intra-utilisateur dans les interfaces cerveau-ordinateur

### Coordonnées

137 rues de Meuniers,  
92220, Bagneux  
0618358529  
Sebvelut28@gmail.com

### Bonjour

Je suis diplômé de l'école d'ingénieur ISAE SUPAERO situé à Toulouse. J'ai découvert le monde de la recherche ainsi que le monde de la neurolA (neuroscience + Intelligence artificielle) lors de mon année de césure à l'ISAE SUPAERO, plus spécifiquement lors de mon stage dans le laboratoire de Frédéric Dehais de NeurolA à l'ISAE SUPAERO. C'est notamment grâce à ce stage que je veus désormais travailler dans le domaine des interface cerveau machine, thème sur lequel portera la thèse que je vais bientôt commencé. Frédéric Dehais est notamment un de mes deux directeur de thèse.

J'ai notamment fait un stage de fin d'année pour finaliser mes trois années à l'ISAE SUPAERO dans une entreprise de, recherche néerlandaise ou j'ai participer à une recherche sur la possibilité de lire les émotions et bien-être d'une personne grâce à des vidéos infrarouges. Ce stage m'a confirmé que je voulais continué mes études par une thèse pour rester dans le monde de la recherche et appronfondir mes connaissances dans le monde de l'intelligence artificielle et de la neuroscience et surtout des interface cerveau machine. J'ai malheureusement demandé trop tard et c'est pourquoi il y a une pause de 1 an entre la fin de mes études et mon début de thèse.

Toutes mes expériences passées et le retour de mes amis en thèse m'ont confirmé dans l'idée de partir sur cette thèse avec Frédéric Dehais et Sylvain Chevalier dont le titre est : *Comprendre et aborder la variabilité intra-utilisateur dans les interfaces cerveau-ordinateur*. Je suis motivé et prêt à travailler et de me donner à fond pour mener à bien cette thèse.

Je vous remercie d'avoir pris le temps de lire cette lettre de motivation. Je suis impatient de vous rencontrer.

Cordialement,

Sébastien Velut

See discussions, stats, and author profiles for this publication at: <https://www.researchgate.net/publication/360619652>

# High frequency stimulations for Steady-States Visual Evoked Potentials (SSVEP)

Presentation · September 2021

CITATIONS  
0

READS  
40

6 authors, including:



**Simon Ladouce**  
Institut Supérieur de l'Aéronautique et de l'Espace (ISAE)

21 PUBLICATIONS 259 CITATIONS

[SEE PROFILE](#)



**Ludovic Darmet**  
ISAE-Supaero

16 PUBLICATIONS 43 CITATIONS

[SEE PROFILE](#)



**Juan Jesús Torre Tresols**  
Institut Supérieur de l'Aéronautique et de l'Espace (ISAE)

15 PUBLICATIONS 653 CITATIONS

[SEE PROFILE](#)



**Sébastien Velut**  
Institut Supérieur de l'Aéronautique et de l'Espace (ISAE)

5 PUBLICATIONS 17 CITATIONS

[SEE PROFILE](#)

Some of the authors of this publication are also working on these related projects:



Human-Robotic Performance [View project](#)



D3CoS - Designing Dynamic Distributed Cooperative Systems [View project](#)

# High frequency stimulations for Steady-States Visual Evoked Potentials (SSVEP)

Simon Ladouce<sup>1</sup>, Ludovic Darmet<sup>1</sup>, Juan J. J. Tresols<sup>1</sup>, Giuseppe Ferraro<sup>1</sup>, Sébastien Velut<sup>1</sup>, and Frederic Dehais<sup>1,2</sup>

<sup>1</sup>ISAE-SUPAERO, Human Factors and Neuroergonomics, Toulouse, 31000, France

<sup>2</sup>Drexel University, School of Biomedical Engineering, Philadelphia, PA, United States

## Introduction and motivation

The Steady-States Evoked Potentials (SSVEP) characterize neural responses to the presentation of periodic visual stimuli, with specific frequency. The sustained rhythmic entrainment of visual cortex neuronal populations to the frequency of the stimuli can be recorded with surface electroencephalography (EEG). Brain Computer Interface (BCI) applications have capitalized on the robustness of the SSVEP effect to achieve unequalled classification performances (e.g., Information Transfer Rate over 300 bits/mins for a 40-class keyboard application) which has further established the SSVEP as a ubiquitous approach for reactive BCIs. Although SSVEP-based paradigms have been proven to be an efficient approach, several concerns regarding the user experience have been raised. More pointedly, the presentation of visual information with flickering rate between 6 to 30Hz has been shown to cause eye strain and may trigger photosensitive epileptic seizures. One potential remedy to improve user experience is to display high frequency stimulus. SSVEP frequencies are typically selected in the 8-20Hz range and some specific studies tried using frequencies up to 30Hz with high luminance intensity LEDs (Kuš et al., 2013). To the best of our knowledge, exploiting frequencies above 30Hz has not been documented yet in the context of BCI, using monitor display. The highest stimulation frequency is limited to half of the monitor refresh rate (Nyquist rate). Typical monitors could only display 60 frames per second limiting the presentation of stimuli to a maximum of 30Hz. The latest generations of computer monitors are characterized by their high refresh rates (i.e., up to 240 frames per seconds) that allow the presentation of higher frequency visual stimuli (up to 120Hz) opening up the use of high frequency stimuli for SSVEP-based BCI applications with better user experience.

## Research question

Due to the aforementioned hardware limitations, the Signal-to-Noise Ratio (SNR) or classification performances of SSVEP-based BCI with stimuli frequencies above 30Hz have not been formally characterized. It is however widely documented that the EEG power spectrum follows a decreasing  $1/f$  law. Although lower SSVEP signal is expected at higher frequencies, variability related to endogenous brain activity (typically recorded at low frequencies) should be less salient. An open question is therefore whether SSVEP responses at higher frequencies have a sufficient SNR to achieve high classification performance.

## Methods and experimental setting

The present study aims to evaluate user experience and characterize SSVEP response elicited across a wide frequency range. To this end, subjective assessment of visual stimuli, SNR of SSVEP responses and classification performances is compared across 24 frequencies ranging from 8 to 60Hz (with a step increase of 2). Neighbouring frequencies to the line noise are excluded (48, 50 and 52Hz). Each frequency is presented alone to avoid confounding factors. We noticed that the elicited response, for example, at 30Hz is different if it is presented simultaneously next to a 8Hz or 60Hz frequency flicker. We used a

standard 10-20 system 32 channel EEG from BrainProducts with a sampling frequency of 500Hz. Signals are band-pass filtered between 1-250Hz. Twelve healthy adults (4 women, mean age: 26 years, range: 21-39 years) with normal or corrected-to-normal vision participated in this study. SNR studies are performed using the Rhythmic Entrainment Source Separation (RESS) methodology (Cohen & Gulbinaite, 2017). We use the state of the art Task Related Component Analysis (Nakanishi et al., 2018) to assess classification performance. A manual selection of electrodes [O1, O2, Oz, P3, P4, Pz, P7, P8] and downsampling to 250Hz is performed for the TRCA algorithm.

#### Results and findings

Preliminary results reveal that the optimal trade-off between SNR/classification performance and user experience is found within the 30-38Hz range. Reported classification accuracy per frequency in Figure 1 suggests that frequency above 42Hz could not be used for a reliable SSVEP-based BCI, as accuracy is below 50% (chance level is 8%). Based on Figure 2, it implies that the maximum subjective comfort score achievable for this pool of subjects is around 7/10. For the 30-38Hz range, participants report a comfort score of approximately 5/10 (see Figure 2) and a classification accuracy of 71.8% (see Figure 1) with 1s epochs. Average accuracy only decreases by -17.4% (from 89.2% to 71.8%) compared to stimuli from the 10-18Hz range. This lower range of frequencies achieves a comfort score of approximately 3/10, really poor in terms of user experience. Thus when using higher frequency, the improvement in terms of comfort for the user is considerable while the classification performances remain acceptable. Beside that and without taking into account user experience, the sweet spot for classification performances and SNR seems to be around 16-18Hz. It is not surprising as more endogenous activity is expected in the lower range of 8-14Hz. Though in Nakanishi et al. TRCA paper they select frequencies between 8 and 16Hz. Our study seems to indicate that their performances could be improved using slightly higher frequencies. The inter-subjects variability is really high with stimuli above 38Hz. For instance for the 40Hz class, and resp. 42Hz, reported classification performances with 1s epochs range from 20% to 100% with standard deviation of 26, resp. 8% and 93% with standard deviation of 27. To compare, standard deviation of the accuracy is only 6 for 16Hz and 1s epochs. The higher ranges provide the higher user comfort but require the setting of an individual threshold for frequency range to counterbalance the inter-subjects variability.

#### Conclusion and future work

This study reveals that higher frequencies (above 30Hz) than usually selected for SSVEP-based BCI could be considered to improve user comfort while keeping a competitive SNR and classification performances. The preliminary results also indicate that frequencies above 42Hz are not reliable, in general as inter-subject variability is significant in this high range, for SSVEP-based BCI.

In our previous work (Ladouce et al., in press), we have shown that reducing amplitude of stimulation also improves user experience of SSVEP-BCI. Reduction of amplitude, with new trade-offs, could be brought together with the use of high frequency. To allow the comparisons in a realistic scenario, further investigations with simultaneous flickering stimulus will be conducted in our future work.

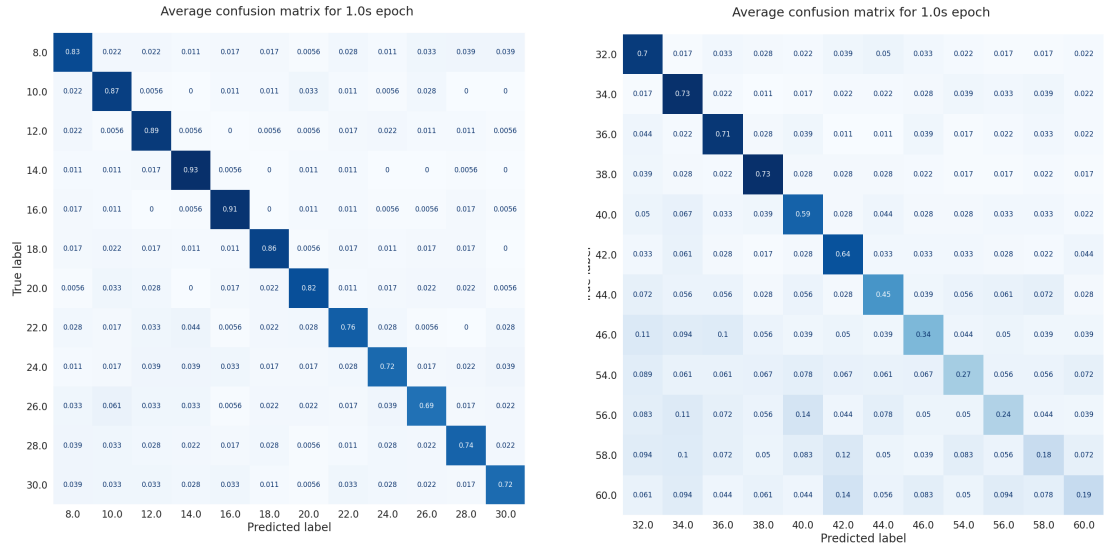


**Figure 1.** Confusion matrices with classification accuracy using TRCA classifier and 1s epoch. Classification accuracy is computed using 5-folds cross validation over 15 trials. We observe some reliable performances until around 40Hz when it starts to decrease. With higher frequencies (plot on the right) the SSVEP frequencies are closer to Nyquist frequency (data are downsampled to 250Hz) thus less band can be used in the filterbank of the TRCA method, which downgrades performance.

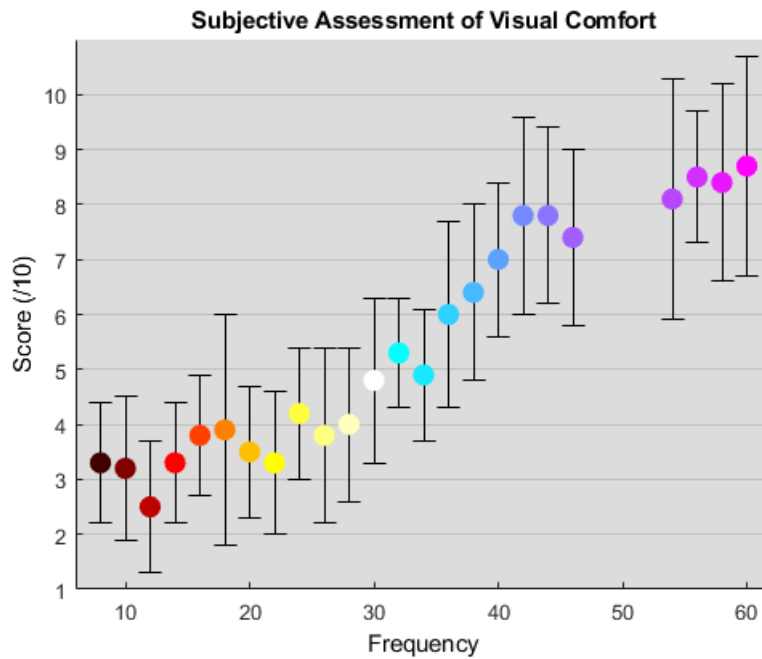


**Figure 2.** Grand average ( $N=12$ ) subjective visual comfort assessment of RVS for each experimental frequency [8-46; 54-60]. The results indicate that visual comfort increases as a function of stimulus frequency. It can be noted that this increase in user visual comfort onsets at 30Hz.

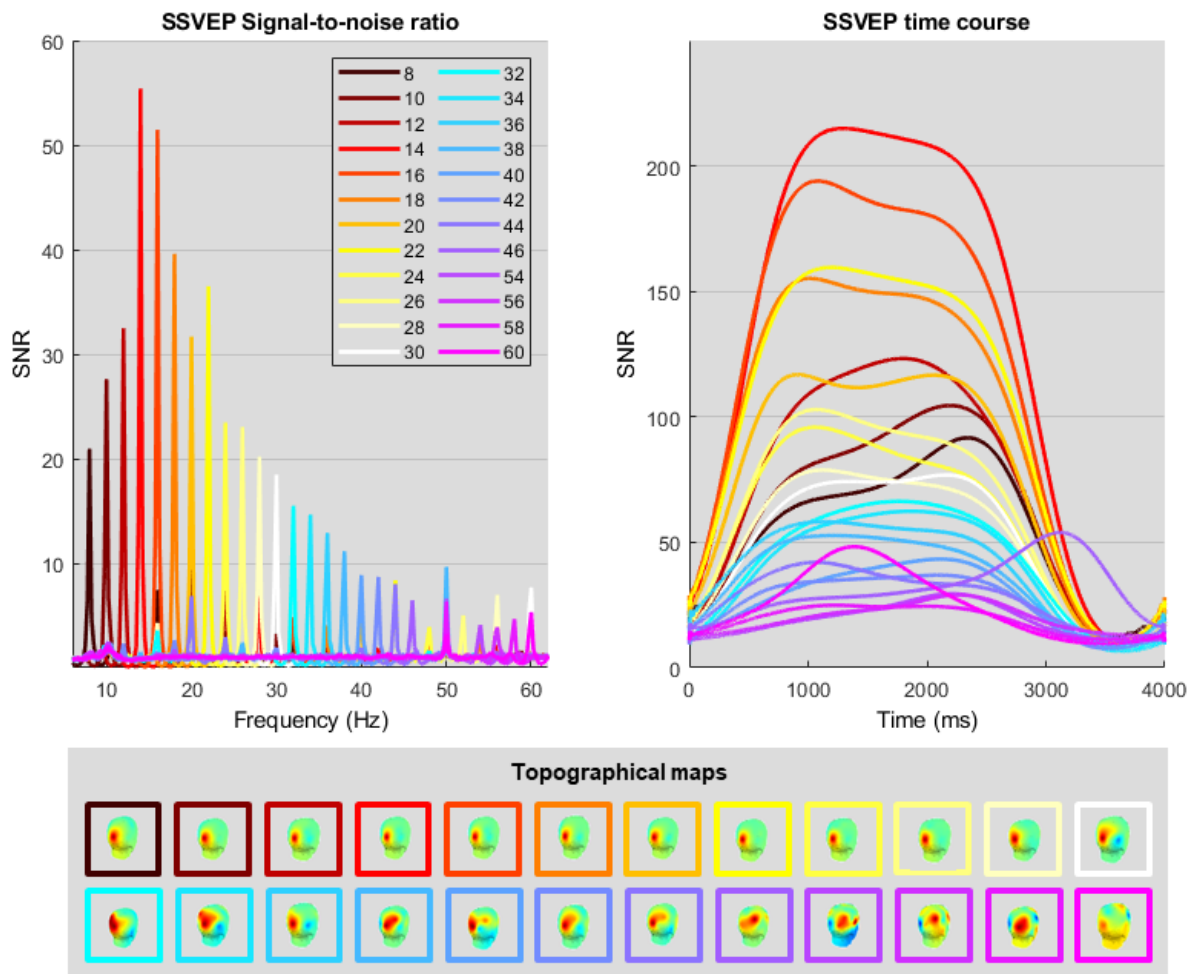


*Figure 3. Top left: Grand average (N=12) Signal-to-Noise Ratio (SNR) of Steady-States Visually Evoked Potentials (SSVEP) responses elicited by each experimental frequency [8-46; 54-60]. Top right: Grand average time course of SSVEP responses. Bottom: Topographical maps representing the spatial distribution of the SSVEP responses. The SSVEP response SNR is maximal within the 16-22Hz range. Following the 14Hz peak, SNR at higher frequencies follows a regular 1/f spectral distribution trend. The prototypical occipital distribution of the SSVEP response is observed up to 44Hz. SSVEP responses elicited by frequencies over 44Hz exhibit lower SNR, unstable time course and high variance of their spatial distribution.*

#### References:

- R. Kuś, A. Duszyk, P. Milanowski, M. Łabęcki, M. Bierzyńska et al. (2013) On the Quantification of SSVEP Frequency Responses in Human EEG in Realistic BCI Conditions. PLOS ONE 8(10)
- M. Nakanishi, Y. Wang, X. Chen, Y. -T. Wang, X. Gao and T. -P. Jung, "Enhancing Detection of SSVEPs for a High-Speed Brain Speller Using Task-Related Component Analysis," in IEEE Transactions on Biomedical Engineering, vol. 65, no. 1, pp. 104-112, Jan. 2018, doi: 10.1109/TBME.2017.2694818.
- M. X. Cohen and R. Gulbinaite, "Rhythmic entrainment source separation: Optimizing analyses of neural responses to rhythmic sensory stimulation" in NeuroImage, vol. 147, pp. 43-56, 2017, doi: 10.1016/j.neuroimage.2016.11.036.

Y . Wang and T. -P. Jung (2010). Visual stimulus design for high-rate SSVEP BCI. *Electronics letters*, 46(15), 1057-1058.

S. Ladouce, J.J. Tresols,L. Darmet, G. Ferraro and F. Dehais (In press). A transparent SSVEP-BCI using low amplitude modulations. IEEE Transactions on Systems, Man, and Cybernetics.

See discussions, stats, and author profiles for this publication at: <https://www.researchgate.net/publication/359866591>

# Dual Passive Reactive Brain-Computer Interface: A Novel Approach to Human-Machine Symbiosis

Article in *Frontiers in Neuroergonomics* · April 2022

DOI: 10.3389/fnrgo.2022.824780

---

CITATIONS

3

READS

122

8 authors, including:



**Frédéric Dehais**  
Institut Supérieur de l'Aéronautique et de l'Espace (ISAE)  
200 PUBLICATIONS 3,659 CITATIONS

[SEE PROFILE](#)



**Simon Ladouce**  
Institut Supérieur de l'Aéronautique et de l'Espace (ISAE)  
21 PUBLICATIONS 259 CITATIONS

[SEE PROFILE](#)



**Ludovic Darmet**  
ISAE-Supaero  
16 PUBLICATIONS 43 CITATIONS

[SEE PROFILE](#)



**Juan Jesús Torre Tresols**  
Institut Supérieur de l'Aéronautique et de l'Espace (ISAE)  
15 PUBLICATIONS 653 CITATIONS

[SEE PROFILE](#)

Some of the authors of this publication are also working on these related projects:



D3CoS - Designing Dynamic Distributed Cooperative Systems [View project](#)



Human-Robotic Performance [View project](#)



# Dual Passive Reactive Brain-Computer Interface: A Novel Approach to Human-Machine Symbiosis

Frédéric Dehais<sup>1,2,3\*</sup>, Simon Ladouce<sup>2</sup>, Ludovic Darmet<sup>2</sup>, Tran-Vu Nong<sup>2</sup>, Giuseppe Ferraro<sup>2</sup>, Juan Torre Tresols<sup>2</sup>, Sébastien Velut<sup>2</sup> and Patrice Labedan<sup>2</sup>

<sup>1</sup> Artificial and Natural Intelligence Toulouse Institute, Université de Toulouse, Toulouse, France, <sup>2</sup> Department for Aerospace Vehicles Design and Control, ISAE-SUPAERO, Université de Toulouse, Toulouse, France, <sup>3</sup> School of Biomedical Engineering, Science and Health Systems, Drexel University, Philadelphia, PA, United States

## OPEN ACCESS

### Edited by:

Caterina Cinel,

University of Essex, United Kingdom

### Reviewed by:

Ranjana K. Mehta,

Texas A&M University, United States

Jordan Navarro,

Université de Lyon, France

### \*Correspondence:

Frédéric Dehais

frédéric.dehais@isae-supapro.fr

### Specialty section:

This article was submitted to

Neurotechnology and Systems

Neuroergonomics,

a section of the journal

Frontiers in Neuroergonomics

Received: 29 November 2021

Accepted: 02 March 2022

Published: 11 April 2022

### Citation:

Dehais F, Ladouce S, Darmet L, Nong T-V, Ferraro G, Torre Tresols J,

Velut S and Labedan P (2022) Dual

Passive Reactive Brain-Computer

Interface: A Novel Approach to

Human-Machine Symbiosis.

Front. Neuroergon. 3:824780.

doi: 10.3389/fnrgo.2022.824780

The present study proposes a novel concept of neuroadaptive technology, namely a dual passive-reactive Brain-Computer Interface (BCI), that enables bi-directional interaction between humans and machines. We have implemented such a system in a realistic flight simulator using the NextMind classification algorithms and framework to decode pilots' intention (reactive BCI) and to infer their level of attention (passive BCI). Twelve pilots used the reactive BCI to perform checklists along with an anti-collision radar monitoring task that was supervised by the passive BCI. The latter simulated an automatic avoidance maneuver when it detected that pilots missed an incoming collision. The reactive BCI reached 100% classification accuracy with a mean reaction time of 1.6 s when exclusively performing the checklist task. Accuracy was up to 98.5% with a mean reaction time of 2.5 s when pilots also had to fly the aircraft and monitor the anti-collision radar. The passive BCI achieved a  $F_1$ -score of 0.94. This first demonstration shows the potential of a dual BCI to improve human-machine teaming which could be applied to a variety of applications.

**Keywords:** passive and reactive Brain Computer Interface, electroencephalography, flight simulator, user experience, Visual Evoked Potential (VEP)

## 1. INTRODUCTION

Brain-Computer Interfaces (BCI) offer a direct communication pathway between a user and a machine without requiring any muscular engagement (Clerc et al., 2016). To this end, BCI derives the user's intentions and mental states from neural signals. The decoding of specific neural signals triggers interactions with aspects of the computerized environment (e.g., moving a cursor, keystrokes) or external devices (e.g., prostheses) to which they are associated with. Its non-invasiveness and high temporal resolution along with its ease of setup and relatively low cost have established surface electroencephalography (EEG) as the most widely used brain imaging method for BCI (Lotte et al., 2018). While BCI was initially developed within the confines of standard

laboratory conditions, recent advances in mobile neurophysiological sensing devices and artificial intelligence have led to a renewed interest in BCI applied to real-world contexts (Fairclough and Lotte, 2020). As a result, these neurotechnologies are now expanding in the clinical field (assistive technologies, motor rehabilitation, etc.), spreading to the entertainment industry to enhance gaming experience, but also extending to the general public through wellbeing (e.g., meditation and relaxation induction, sleep improvement) and domotics (e.g., home automation) applications (Brouwer, 2021). Following this trend, the range of neuroergonomics applications that can benefit from BCI broadens as sensors and interfaces become ever less intrusive (Dehais et al., 2020a; Gramann et al., 2021). Indeed, BCI has the potential to alleviate mental and physical loads associated with the repetition of straining actions (Carelli et al., 2017; Maksimenko et al., 2018), to improve task performance both in terms of its precision and speed, and to promote new forms of interactions to enhance human-machine teaming (Dehais et al., 2020b). Such assistance is particularly desirable in the context of aircraft operations. Flying a plane is a highly demanding task from a cognitive standpoint since it takes place in a dynamic and uncertain environment. It is well-established in cognitive science literature that attentional resources are limited (Kahneman, 1973). This limited capacity implies that the pool of cognitive resources has to be distributed across competing sensory modalities (Wickens, 2008). The amount of cognitive resources available at any given time is also mediated by other factors such as stress and mental fatigue. Following prolonged periods requiring attentional focus, individuals typically exhibit performance decline as fatigue ensues (Dehais et al., 2018). Pilots have to attend to and assess several sources of visual and auditory information spread around the cockpit, and have to take decisions under time pressure and execute maneuvers in a timely manner (Wickens and Dehais, 2019; Behrend and Dehais, 2020). The combination of the stress-inducing context of flight operations and the need to sustain attentional focus over long periods of time is particularly taxing and tiring for pilots. The accumulation of mental fatigue and stress hinders access to the pool of cognitive resources (Hancock and Szalma, 2008), which in turn can lead to completely overlooking information (e.g., attentional tunneling). This phenomenon has been observed in experienced pilots and can have dramatic consequences (Wickens and Alexander, 2009; Dehais et al., 2019a; Mumaw et al., 2019). The on-line estimation of pilots' monitoring ability combined with implementing new types of interactions through neuro-adaptive technologies may therefore have critical implications for flight safety.

There are several ways whereby BCI can enhance pilot-cockpit teaming. Firstly, active and reactive BCIs allow users to perform interactions under voluntary control *via* their brain waves (Hong and Khan, 2017; Lotte and Roy, 2019). Several studies disclosed that such technology can be used by pilot to control the flight-path of airplanes and drones (Fricke et al., 2014; Nourmohammadi et al., 2018; Rodriguez-Bermudez et al., 2019). Active BCI require the users to deliberately produce brain signals to interact with the BCI, as with mental imagery. In contrast, reactive BCI (rBCI) makes advantage of the user's

cerebral responses elicited by different stimuli. Each stimuli is associated with a different command. Due to their robustness and quick onset (i.e., below 50 ms), the Visual Evoked Potentials (VEP) elicited through the presentation of modulated visual stimuli are a popular and efficient approach for rBCI (Zhu et al., 2010; Chevallier et al., 2021). They offer very high classification performance (Nakanishi et al., 2018; Nagel and Spüler, 2019). Neural activity recorded in the visual cortex with surface EEG is sensitive to temporal and frequency features of the visual stimuli. Two main types of VEP-based paradigms can be distinguished: Steady-States Visually Evoked Potentials (SSVEP) and code-Visually Evoked Potentials (c-VEP). While SSVEP consists of the periodic modulation of visual features (e.g., contrast, color) at a regular frequency sustained over time, c-VEP waveforms are generated by pseudo-random binary (on/off) sequences. The c-VEP pseudo-random sequences are usually broadband and aperiodic (Shirzhiyan et al., 2019). They are defined so that temporal shifts have minimum cross-correlation and ensure a good separation between classes. VEP-based paradigms present the main advantage of relatively short training time, compared to P300 ERP or Motor Imagery paradigms, as only a low number of short-lasting trials is usually required to achieve accurate calibration (Nagel and Spüler, 2019). In the field of aviation, visual BCI could offer promising perspectives for pilots by allowing them to free their hands when interacting with some actuators (e.g., landing gear, flaps). This could be particularly relevant during high g-force scenarios or critical flight phases (e.g., low altitude situations) that require both hands to control the stick and the thrust.

A second approach to improve pilot-cockpit teaming is to consider the use of passive BCIs (pBCI). This latter type of neuroadaptive technology supports implicit interaction by monitoring mental states (e.g., stress, fatigue) and adapting human-machine interactions to overcome cognitive bottlenecks (Zander and Kothe, 2011; Ewing et al., 2016). Several pBCI studies have been implemented in the field of aviation to infer mental workload (Gateau et al., 2018; Dehais et al., 2019a), failure of attention (Dehais et al., 2019b,c), flying performance (Scholl et al., 2016; Klaproth et al., 2020), and mental fatigue (Dehais et al., 2018). Interestingly enough, some authors managed to close the loop by triggering adaptive automation to prevent mental overload and task disengagement (Prinzel et al., 2000; Aricò et al., 2016). Generally, specific frequency-domain features are computed over the electrophysiological signal to account for different mental states (for a review, see Borghini et al., 2014). For instance, changes in mental demand are related to the variation in the alpha band power and in theta band power over fronto-parietal sites (for a review, see Borghini et al., 2014). Some studies also disclosed that increased beta (Matthews et al., 2017) is a neural marker of higher mental efforts. Alternatively, time-domain analyses over the EEG signal (i.e., event-related potential) can also predict variations of cognitive performance and attentional states (Brouwer et al., 2012; Roy et al., 2016; Dehais et al., 2018). One major drawback of such approach is that the calibration requires the induction of the mental states (e.g., different levels of stress or attention) in a repetitive fashion to train the model. It is difficult to achieve under laboratory

conditions and, more importantly, is detrimental to the user experience. One alternative approach would be to take advantage of VEP and to use code-VEP tagging stimuli to implement a pBCI. By placing these flickers within the background of different regions of interest, one can measure the intensity of the brain response and derive the level of attention allocated to these specific areas.

Taken together, all these studies demonstrate the benefit of rBCI and pBCI to improve pilot-cockpit teaming and flight safety. However the rBCI and pBCI technologies to date have been used separately, whereas many of everyday-life tasks involved conjointly some voluntary interactions with a user interface and the monitoring of the state of the machine. Moreover, the same device (e.g., EEG) could be used to collect brain data and feed different algorithms in charge to control an interface and to infer the user mental state. Such an approach would pave the way to design a novel concept of neuroadaptive technology, namely a dual BCI (dBCI). By “dual,” we mean that it combines both “reactive” and “passive” components of the BCI to support direct and implicit interactions for end-users. This approach echoes with the concept of invasive bidirectional BCI for disable people that have been designed to translate motor cortex activity into signals to control an apparatus and to provide feedback by translating artificial sensor to restore sense of touch (Hughes et al., 2020). In our case, the dBCI relies on a non-invasive technology such as surface electrodes placed over the scalp (i) to allow an end-user to directly control a machine through their brain activity and (ii) to allow a machine to communicate feedback to its end-user and thus adapt human-machine interaction to overcome cognitive bottleneck.

The objective of this study was to implement such a dBCI in the cockpit. To meet this goal, we used the NextMind 9-electrode dry EEG system and their Unity framework ([www.next-mind.com](http://www.next-mind.com)) that allows to implement asynchronous code-VEP based BCI for up to 10-class problems. We chose the NextMind as their hardware is light, fast to setup, and the classification is plug-and-play but this could have been done with another BCI system. Our main motivation was not to focus on the algorithmic implementation but to demonstrate the effectiveness of our genuine dBCI to decode pilots’ intention to interact with the flightdeck (reactive, rBCI) and to infer their level of attention on a monitoring task and to adapt the interaction accordingly (passive, pBCI, see **Figure 1**).

The designed scenario in the flight simulator requires to tackle both direct (rBCI) and implicit (pBCI) interactions. Indeed, the participants had to perform several checklists operated through rBCI and a radar monitoring task which was handled by the pBCI while completing an engaging traffic pattern exercise. We evaluated the rBCI during two contrasted experimental conditions in terms of task difficulty. In one condition, the participants were interacting with the rBCI alone while the plane was operated by the autopilot. In another condition, they were operating the rBCI while flying the plane and monitoring the radar. We collected objective measures (reaction time and accuracy) and subjective measures (level of mental demand and frustration). It was expected that the multitasking condition would lead to longer reaction times to interact with the rBCI,

more frustration and lower accuracy. We evaluated the pBCI component using classical machine learning metrics ( $F_1$  score, sensitivity, and specificity).

## 2. MATERIALS AND METHODS

### 2.1. Participants

Twelve participants (one female, mean age = 29.8 year old and SD = 7.4, mean flight hours = 488.9, and SD = 115.7), all students and staff members from our aeronautical university, took part in the experiment. The study was approved by the Local Ethics Committee (approval number 2020 – 334). We followed specific COVID procedures implemented by our Health, Safety, and Working Conditions Committee (anti-COVID face masks, sanitization of the flight simulator, disinfection of the eye tracker, and EEG device following a thorough cleaning procedure).

### 2.2. Dual BCI Implementation

We used the NextMind Unity Software Development Toolkit (SDK)<sup>1</sup> to implement the rBCI and the pBCI. An MSI laptop (processor Intel i7 – 6700HQ with 16 GB RAM and NVIDIA GeForce GTX 960M graphic card) was used to receive the EEG data stream through Bluetooth Low Energy. This PC executed the decoding algorithms and sent the decoded brain command to the core simulator via socket TCP/IP (using an Ethernet connection) that consisted of a thread of four commands (integer type) to change the states of the flaps, the landing gear, the landing and taxi lights and the autopilot (see **Figures 1, 2**). Since the NextMind is a closed system, it does not provide direct access to the processing time for the classification. However, we managed to estimate the pace of update for the classification output, before it is displayed (to avoid a bias with the refresh rate of the screen). Our measures indicated that the framework takes in average 10.38 ms (SD = 0.05 ms) to refresh the classification score.

#### 2.2.1. rBCI

The rBCI display consisted of four toggle switches (diameter = 4cm) that are defined as “Neurotag” interactive elements (i.e., a NextMind code-VEP) in Unity. They are depicted in the upper left part of **Figure 1**, outlined in red. These switches are dedicated to lower/retract the flaps, switch on/switch off the taxi and landing lights, to lower/retract the landing gears and to engage/disengage the autopilot system (see **Figure 2**, left).

#### 2.2.2. pBCI

For the pBCI, the region of interest was a radar. We have integrated a “Neurotag” (diameter = 13.1 cm) in the background. It is depicted in the lower left part of **Figure 1**, outlined in blue. The brain response to this background c-VEP was used to assess the level of attention of the pilot to the region. Thus, instead of using the regular rBCI classification procedure, we have taken advantage of a continuous *confidence score* ( $\in [0, 1]$ ) defined by the NextMind Engine as a proxy measure for attention to the radar. This score reflects the classification certainty for a rBCI. If this score was too low and a collision was incoming, our system would infer that the pilot is not paying attention at the

<sup>1</sup><https://www.next-mind.com/developer>

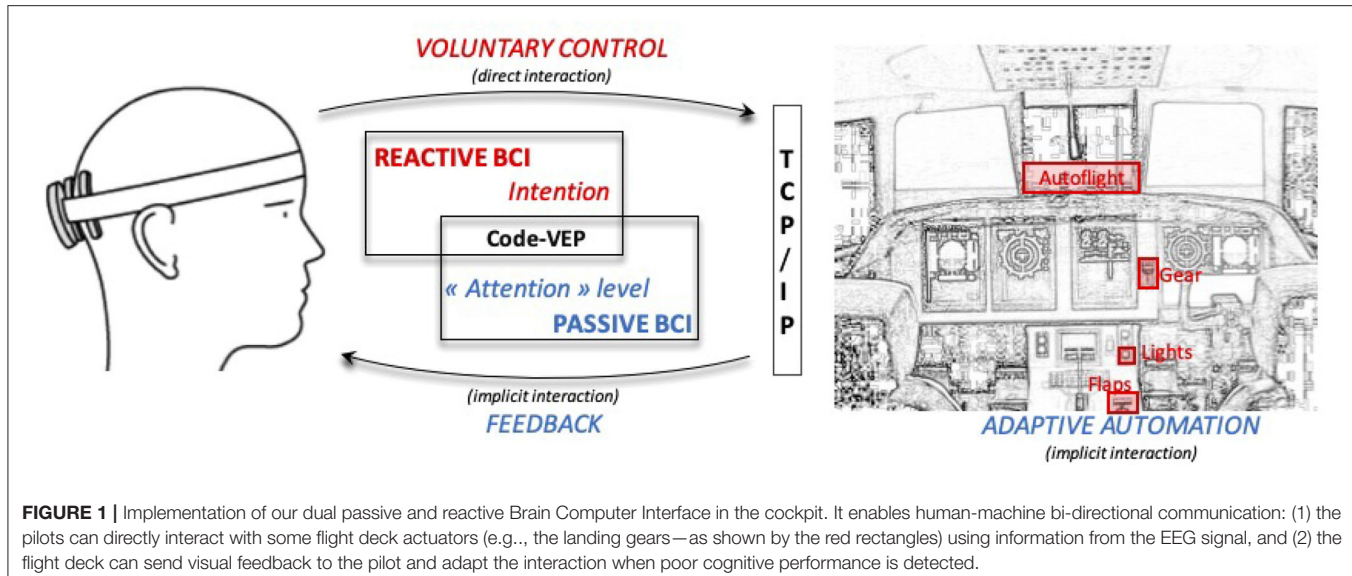


**FIGURE 1 |** Implementation of our dual passive and reactive Brain Computer Interface in the cockpit. It enables human-machine bi-directional communication: (1) the pilots can directly interact with some flight deck actuators (e.g., the landing gears—as shown by the red rectangles) using information from the EEG signal, and (2) the flight deck can send visual feedback to the pilot and adapt the interaction when poor cognitive performance is detected.

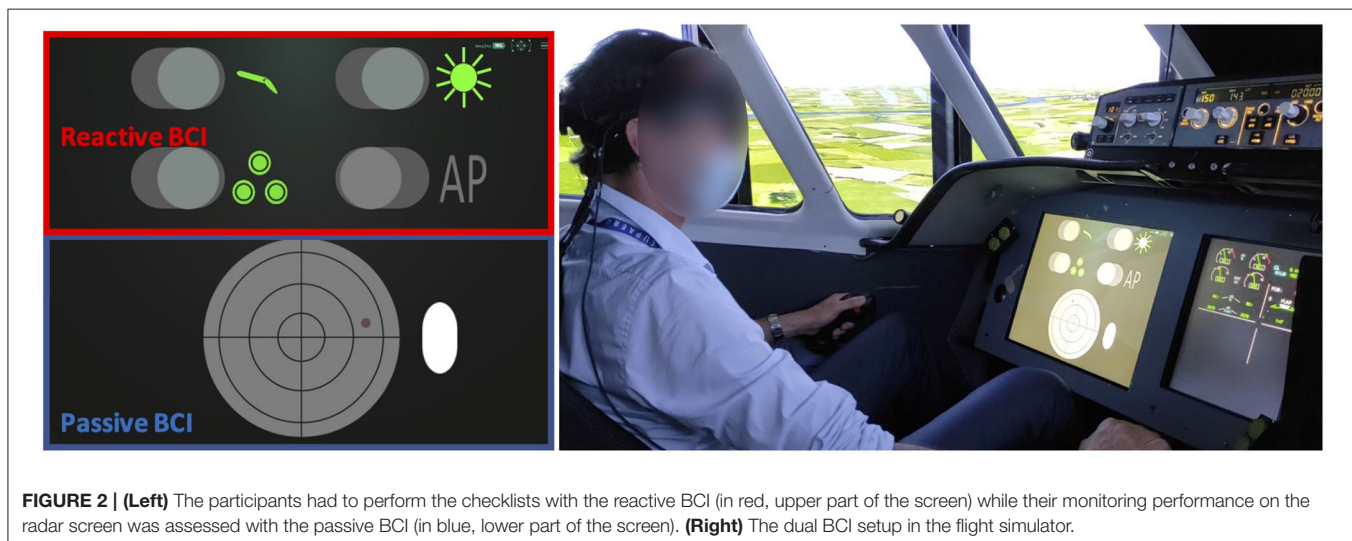


**FIGURE 2 | (Left)** The participants had to perform the checklists with the reactive BCI (in red, upper part of the screen) while their monitoring performance on the radar screen was assessed with the passive BCI (in blue, lower part of the screen). **(Right)** The dual BCI setup in the flight simulator.

radar and therefore not able to avoid the collision. It would then automatically activate the anti-collision maneuver and trigger an orange visual alert (see **Figure 3**). Based on a preliminary experiment with 5 participants, we set a threshold of 0.1 on the *confidence score* to have good responsiveness to determine whether the pilots were actually monitoring the anti-collision radar or not (see **Figure 2**, right). The classification processes are different between the rBCI (regular and hard decision of classification) and the pBCI (the certainty of classification by the model as attention probe), though they both use the response to the same type of c-VEP as input.

### 2.3. Flight Simulator

We used our three-axis hydraulic (pitch, roll, height) motion flight simulator to conduct the experiments. It has eight external panoramic displays that reproduces the outside world based

on the Flight-Gear open-source software.<sup>2</sup> It simulates twin-engine aircraft equipped with two side-sticks, a thrust, two rudders, and an advanced auto flight system (**Figure 2**). Its user interface is composed of a Primary Flight Display, a Navigation Display, and an Electronic Central Aircraft Monitoring Display and a head-up-display (HUD). The HUD provides basic flight parameters (speed vector, angle of attack, total energy) and thus allows the pilots to control the flight path and the speed of the airplane. The flight simulator refreshes every 20 ms the inputs from the BCI system sent through the TCP/IP connection, in addition to the information coming from the traditional organs of piloting like the autopilot button, the flaps and landing gear levers, etc. The dual-BCI user interface (checklists and anti-collision radar) was displayed on a head down 17" screen

<sup>2</sup>[www.flightgear.org](http://www.flightgear.org)

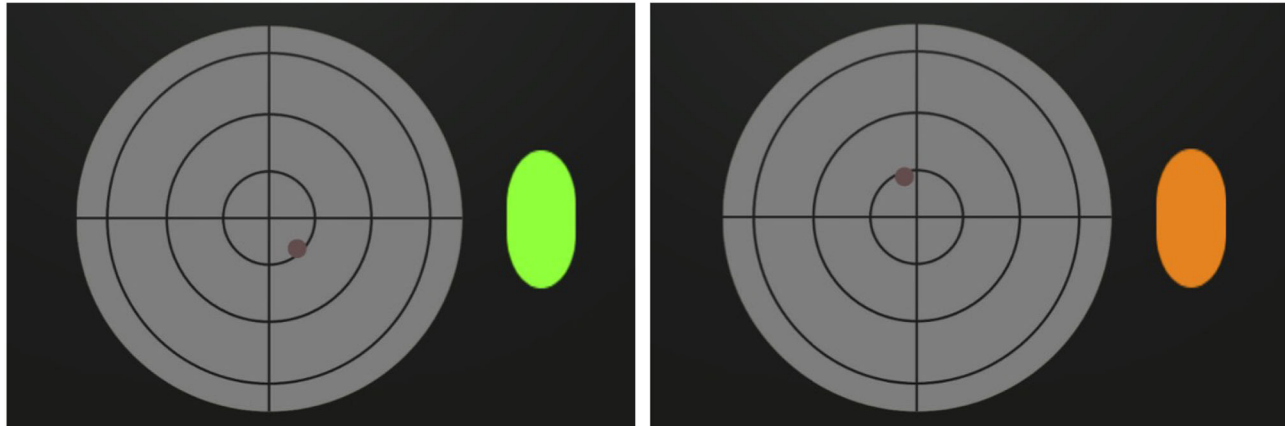


**FIGURE 3 | (Left)** The pBCI detected that the pilot was correctly monitoring the radar and, in return, displayed a green visual feedback. **(Right)** The pBCI detected that the pilot did not notice the potential collision. It then displayed an orange warning and automatically simulated the avoidance maneuver.

( $1,280 \times 1,024$ –60 Hz) facing the participants (head distance = 80 cm).

## 2.4. Scenario

We have designed a scenario in which the participants had to perform two checklists (rBCI) and a radar monitoring task (pBCI). The flying task consists of a first landing at Toulouse Blagnac runway (33R) followed by a go-around, then a traffic pattern exercise leading to a final landing. The participants had to use the rBCI during the:

1. **first landing:** to lower the gear, to lower the flaps, to switch on the landing and taxi lights;
2. **go-around:** to retract the gear, to retract the flaps, to switch off the taxi and landing lights and to engage the autopilot;
3. **crosswind:** to disconnect the autopilot;
4. **downwind:** to lower the flaps and to switch on the lights;
5. **final landing:** to lower the landing gear.

The four items of the checklist did not demand immediate responses but their correct activation/deactivation is of critical importance during the execution of the traffic pattern, as specified by the standard operational procedures. As depicted in **Figure 1** these actuators (in red) were located out of reached from the left-seated participant-pilot and any interactions with them require torso movements and arm extension. Our objective was to show that a reactive BCI could allow the pilots to keep their hands on the stick and thrust lever while performing the required check-lists.

Meanwhile and while flying the plane, participants should monitor the anti-collision radar (pBCI). The anti-collision task was not performed in the auto-pilot condition (low workload) but only while flying (high workload). The collisions were not linked to the actual flight pattern exercise and only appeared on the radar. In practice, it implies looking frequently at this radar to determine if another plane (represented by a red circle) reaches the center of the radar, indicating a collision within 6 s. In the case of an incoming collision, pilots were asked to focus on the radar. This would mean that they have acknowledged

it and would avoid it. When a collision is incoming, an anti-collision system would be triggered by the pBCI either by (i) the detection of sufficient attention to the radar (ii) or by the detection of inattention of the pilot. With this scenario, the expertise of the pilot to avoid collisions is primary and it is bypassed only if the system estimated that the pilot is distracted. It is different to a scenario that would systematically activate the anti-collision manoeuvre, which sets aside the pilot assessment of the situation. Thus, the idea of this pBCI is to offer supplementary assistance to the pilot during overwhelming situations but not to automate his or her tasks. It is worth noting that we artificially increased the number of potential collisions compared to what pilots are expected to face during real operations for the purpose of the study. The goal was to have enough events of missed collisions so as to have statistically significant results without substantially extending the experiment duration.

In order to assess the effect of mental workload and multitasking on the use of rBCI, we manipulated two variations of the experimental conditions:

- **rBCI alone condition (single task condition):** the participants only had to perform the different checklists without flying (the aircraft was in automated flight mode). They also did not have to do the anti-collision monitoring task;
- **r/pBCI and Flying condition (multi-tasks condition):** the participants had to perform the checklists and the radar monitoring task while manually flying to perform the five legs of the scenario.

These stand for two realistic conditions of flight: auto-pilot mode and full control. A video that illustrates the experimental scenario can be downloaded in the **Supplementary Materials**.

## 2.5. Protocol

The participants underwent 30 min of training for the flight simulator without the dBCI. It included a short tutorial about how the simulator worked (user interface, flight parameters),

several landings and a complete traffic pattern exercise. Participants were then equipped with the 9-electrode NextMind EEG headset (Oz, PO7, PO8, PO1, PO3, PO4, P3, P4), placed over the visual cortex with the lowest electrode (Oz) set over the inion, as recommended by the manufacturer best practices.<sup>3</sup> Following this, participants went through the BCI calibration phase which output a calibration score (between 1 and 5). During the calibration phase, the participant had to focus on a single c-VEP for 40 s. The calibration was redone if the score was below 4 to ensure satisfactory performances. After this setup, participants completed the two conditions (rBCI alone and r/pBCI + flying). The order of the two conditions was pseudo-randomized to counterbalance between all participants and to control for potential fatigue effects: six participants started with the “rBCI alone” condition and the remaining six with “r/pBCI and flying” condition. Finally, after completing each experimental condition, participants were asked to fill the subjective questionnaire. The total length of the experiment for a subject was about 1 h.

## 2.6. Measurements

### 2.6.1. Subjective Measures

The participants reported their subjective levels of mental effort and frustration to perform the checklists using a Likert scale (1 = very low, 10 = very high) in the two experimental conditions. These subjective assessments were done immediately after completing the experiments.

### 2.6.2. Objective Measures

We used *a posteriori* the recording from a Tobii Glasses II eye tracking system (Tobii Pro AB, Stockholm, Sweden) to manually evaluate the efficiency of the dBCI system. Tobii Glasses II is a wearable eye tracker with an embedded scene camera of frequency 60 Hz (i.e., a sampling interval of 16.67 ms). The recording consists in the video of the scene camera, with a large angle, with in overlay the gaze point of the subject. Built-in parallax and slippage compensation methods were performed to maintain tracking accuracy throughout the recording. During the calibration procedure a target probe was presented in the cockpit. During recording, if the gap between two retrieved samples was more than 16.67 ms and <75 ms, the sample is considered as missed. Missed samples were interpolated using the median on a rolling window of five samples. If the gap is more than 75 ms, the samples were considered lost and not interpolated. The proportion of missed and lost gaze samples was bellow 20% for all the participants. The continuous eye-tracking sequences were then smoothed using a non-weighted moving median filter with a window size of three samples. The built-in Tobii I-VT Fixation Filter was set with a velocity (expressed in visual degrees per second) threshold of 30°/s over 20 ms window length. Gaze samples above the velocity threshold were classified as saccade samples. Short fixations lasting <50 ms were discarded. Adjacent short fixations were merged when their inter-fixation (saccade) duration was lower than 75 ms or that the visual angle difference between these fixations was lower than 0.5°. A lower threshold of 200 ms was used for the definition of visual fixations. The

eye tracker is not part of the dBCI system. The recording was used (i) to compute the accuracy of the rBCI and measure the reaction time to perform the checklist events, and (ii) to quantify the performance of the pBCI as follow:

Regarding the reactive BCI:

- A “true positive” was labeled if the participant gazed at one of the checklist item and this latter is then activated/deactivated by the NextMind classification framework;
- A “false positive” was labeled if the state of one checklist item changed without any eye fixation on it;
- The reaction time to interact with checklist item was computed by measuring the time interval from the first fixation on this item until this latter is finally activated/deactivated by the NextMind classification framework;

Regarding the passive BCI:

- A “true positive” was labeled if the participant gazed at the radar and the confident score computed by the NextMind algorithm reached a value of 0.1 within the last 6 s, defined as the time to avoid the collision;
- A “false negative” was labeled if the participant did gaze at the radar but the confident score did not reach a value of 0.1 within the 6 s;
- A “false positive” was labeled if the participant did not gaze at the radar but the confident score reached a value of 0.1 within the last 6 s.

## 3. RESULTS

In this section, we present the subjective and quantitative results of our dual (reactive and passive) BCI.

### 3.1. Subjective Results

A paired t-test ( $p < 0.001$ ) demonstrated that the mean level of frustration to interact with the checklist items was significantly lower in the “rBCI alone” condition (mean = 2.6, SD = 2.0) than in the “r/pBCI and flying” condition (mean = 4, SD = 2.2). Similarly, a paired t-test ( $p < 0.001$ ) demonstrated that the mean level of mental workload to interact with the checklist items was significantly lower in the “rBCI alone” condition (mean = 2.2, SD = 1.4) than in the “rBCI and flying” condition (mean = 5, SD = 2.0, see Figure 4). Such reported results were expected as the “rBCI and flying” is way more demanding compared to “rBCI alone.” We selected these two conditions as they represent two classical flight situations: auto-pilot with low workload and flying with high workload.

### 3.2. rBCI Objective Results

In the “rBCI alone” condition, the classification accuracy reached 100% since all the participants interacted successfully with the checklist items without experiencing any false positives (i.e., activation of an undesired item). Unlike a traditional rBCI with a fixed epoch length, here the epoch length varies. In the “r/pBCI and flying” condition, all the participants managed to fly the different legs of the aircraft while interacting with the different checklist items. The classification accuracy reached 98.5% since

<sup>3</sup><https://www.next-mind.com/documentation/sensor-manual/>

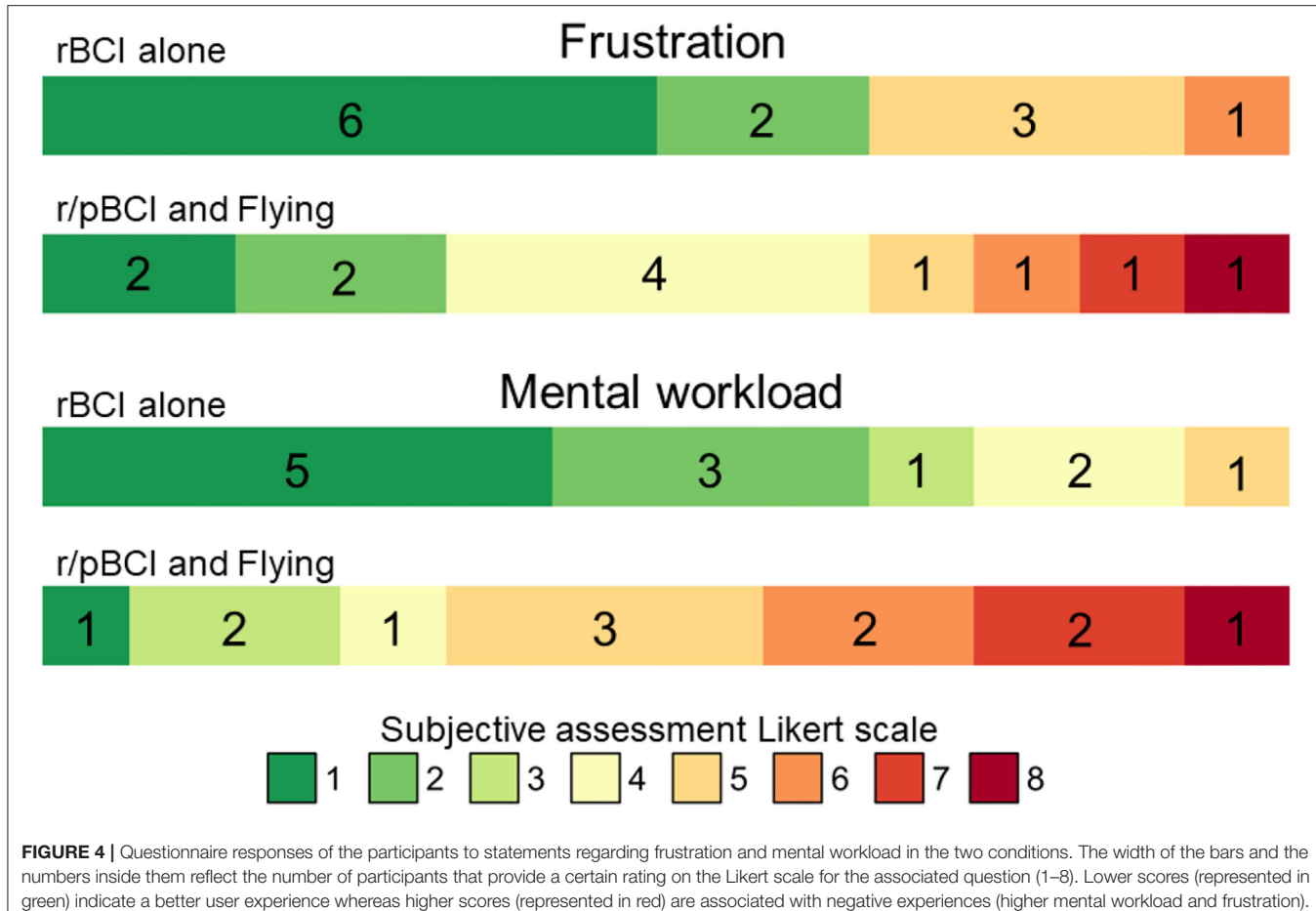


**FIGURE 4 |** Questionnaire responses of the participants to statements regarding frustration and mental workload in the two conditions. The width of the bars and the numbers inside them reflect the number of participants that provide a certain rating on the Likert scale for the associated question (1–8). Lower scores (represented in green) indicate a better user experience whereas higher scores (represented in red) are associated with negative experiences (higher mental workload and frustration).

only two single false positives occurred out of 132 trials (i.e., 11 checklist items  $\times$  12 pilots).

A paired t-test indicated that the mean reaction time to activate the checklist items was significantly lower ( $p = 0.002$ ) when interacting with the rBCI alone (mean = 1643.7 ms, SD = 390.6 ms) than when interacting with the rBCI while flying and monitoring the radar task (mean = 2493.1 ms, SD = 1055.4 ms). Mean reaction times per participant can be found in **Figure 5**.

### 3.3. pBCI Objective Results

The pBCI system have classified as missed by the pilots, a total of 53 potential collisions out of 203 events. Among these 53 missed collisions, the recordings from the eye tracker, manually examined, showed us that in nine cases, the pilot was actually fixating the radar but the pBCI considered as an attentional lapses (False Negative, FN). For the remaining 44 cases (True Negative, TN) and still based on the manual study of the recordings from the eye tracker, the pBCI had accurately detected that the pilot was distracted and compensated attention errors by automatically triggering the orange alert. These results are summarized in **Figure 6**. During the *post-hoc* analysis, we have also determined that in eight cases among the 150 potential collisions classified by the pBCI as acknowledged by the pilots,

but the eye tracker disclosed that the participants were not actually paying attention (False Positive, FP). Therefore it makes a total of  $150 - 8 = 142$  true positives (TP). As such, the True Positive Rate (TPR, also called recall =  $\frac{TP}{TP+FN}$ ) of the pBCI system was 94.04%. The precision ( $\frac{TP}{TP+FP}$ ) was 94.67% and it gives a  $F_1$ -score (harmonic mean of precision and recall) of 0.94. The  $F_1$ -score reflects the number of false positives and negatives along the true positives and negatives while traditional classification accuracy only provides information about true positives and negatives. Within our framework, missing a collision could have dramatic consequences, thus it was more informative to consider  $F_1$ -score than accuracy. The True Negative Rate (TNR, also called selectivity =  $\frac{TN}{TN+FP}$ ) was 84.61%.

## 4. DISCUSSION

This study is the first demonstration of a dBCI system that promotes direct (rBCI) and implicit (pBCI) interaction between the user and the interface. In our task, the reactive and passive aspect did not interact together but were motivated by the task involving interactions with the flight deck and the monitoring of the radar screen. More specifically, the rBCI component allowed the participants to interact with the flight simulator, sending commands through a TCP/IP connection, to change

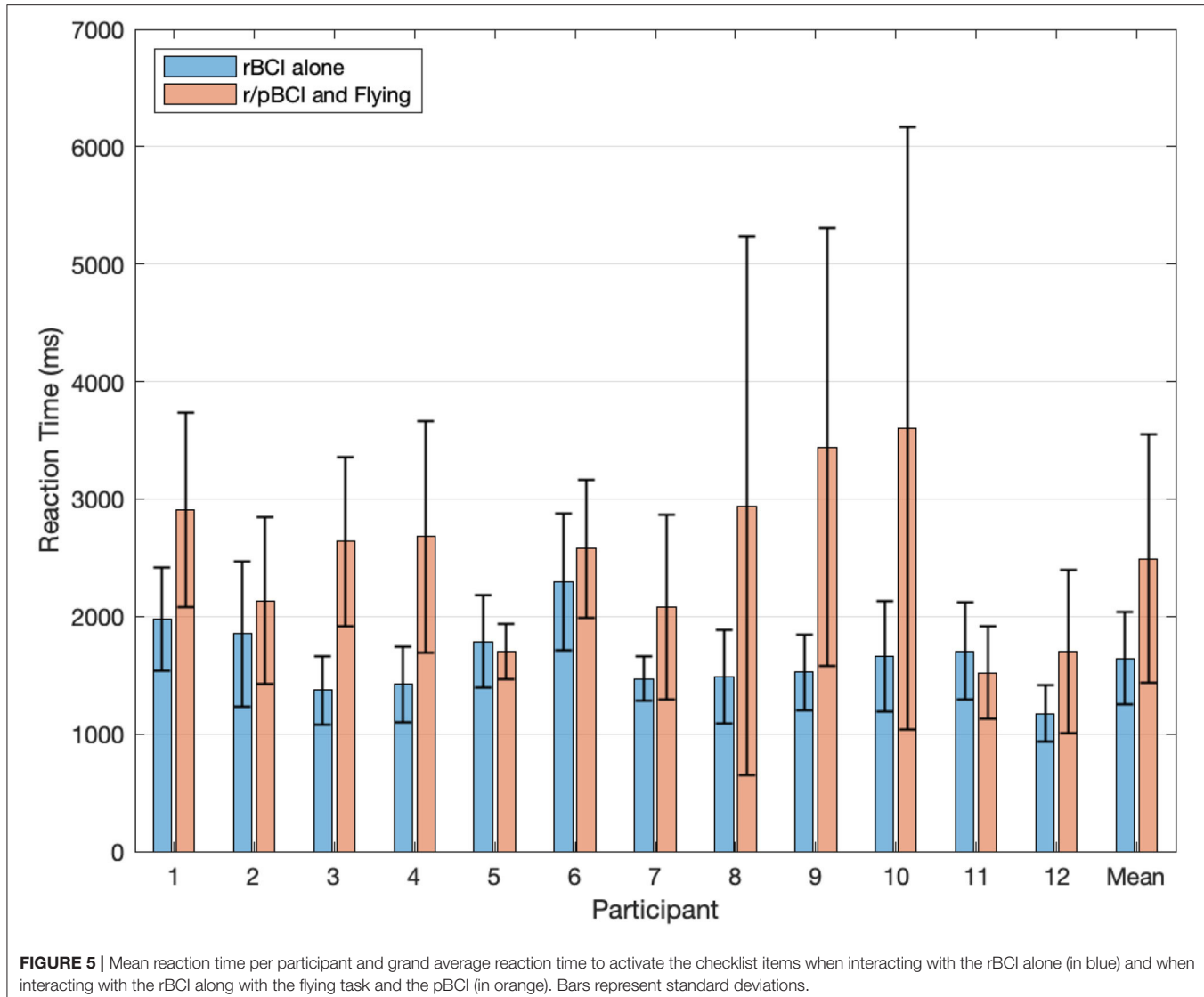


**FIGURE 5 |** Mean reaction time per participant and grand average reaction time to activate the checklist items when interacting with the rBCI alone (in blue) and when interacting with the rBCI along with the flying task and the pBCI (in orange). Bars represent standard deviations.

the state of specific flight deck actuators. This approach differs from previous aviation-oriented BCI studies, which apply BCI to directly control the aircraft's trajectory (Fricke et al., 2014; Nourmohammadi et al., 2018; Rodriguez-Bermudez et al., 2019). It is important to note that in all these previous studies, the pilots were required to fully allocate attentional resources toward the BCI interface in order to perform the flying task whereas the flight performance under the BCI condition does not meet the standards of manual flying accuracy. Another important consideration is that operating an aircraft requires to constantly monitor a rich flow of information distributed across the cockpit. Therefore such artificial setups in which pilots only pay attention to a single source of information does not accurately reflect real-flight situations and may not be transferable to these use cases. Moreover, any relevant secondary task (e.g., radar monitoring, communication with air traffic control) or critical stimuli (e.g., alarms) will distract them from flying. The pBCI component was precisely dedicated to assist the pilot when performing a

secondary task, namely monitoring an anti-collision radar task. To the authors' best knowledge, this is the first time that a VEP is used to monitor attention. Traditionally, this is performed using frequency and/or time-domain features to assess the level of attention (Brouwer et al., 2012; Dehais et al., 2018).

The rBCI analyses disclosed state of the art results in the control condition (auto-pilot) with an accuracy of 100% and a average reaction time of 1.6 s. It should be compared with other asynchronous, online and with 4 classes BCIs of the literature. Kalunga et al. (2016) have reported a reaction time of 1.1 for a 3 class problem and an accuracy of 87.3% for they asynchronous and online BCI. In Gembler et al. (2020), authors have achieved a reaction time of 2.31 s for a 4 class problem and a mean accuracy of 94.4%, also online and asynchronous. The rBCI also led to very high accuracy (98.5%) in the condition where the participants had to operate it while flying the plane and monitoring the radar. The mean reaction was longer but quite acceptable (2.5 s) and allowed the pilots to perform the checklist in a timely manner

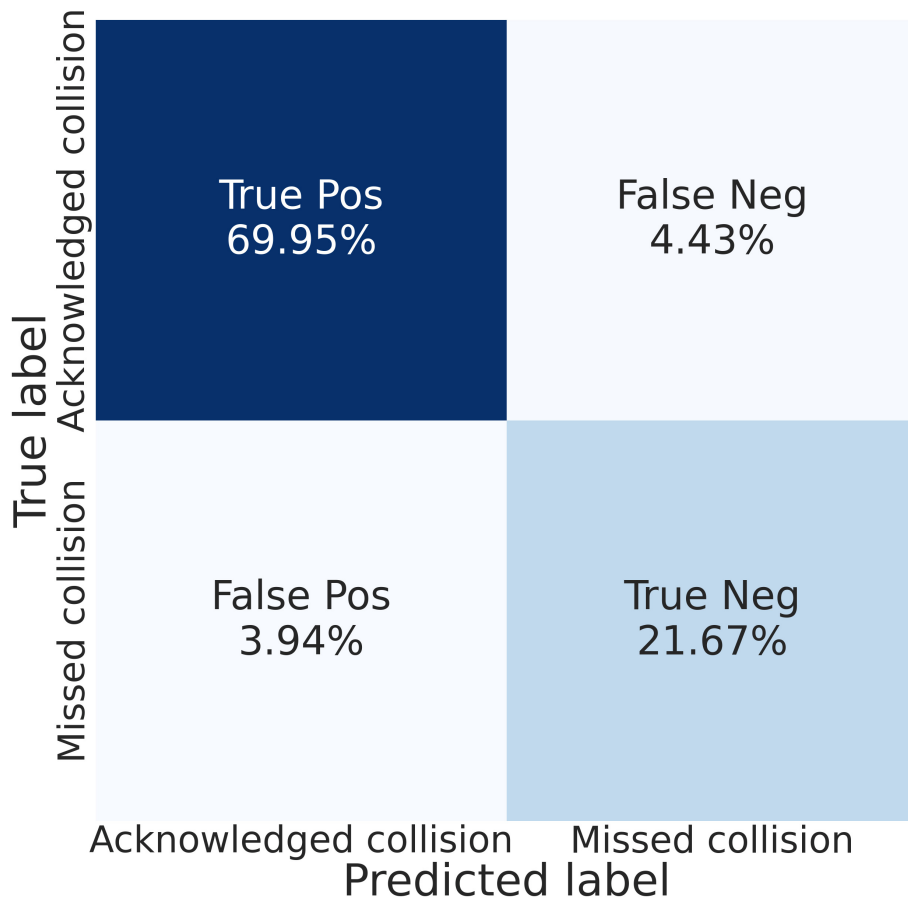


**FIGURE 6 |** Confusion matrix for the pBCI. The ground truth was obtained using *post-hoc* manual analysis of the recordings from the eye tracker. Acknowledged collision corresponds to a collision actually spotted on time by the pilot.

while still being able to navigate and safely land the plane. This slight decrease in classification accuracy ( $-1.5\%$ ) and increase in reaction time ( $+0.9$  s) can be explained in terms of higher mental demand as previously demonstrated by Vecchiato et al. (2016). Indeed, the participants were engaged in a complex multitasking activity, leading them to divide their visual attentional resources between the flying, the radar, and the rBCI tasks. Our subjective results seemed to confirm this hypothesis as our participants expressed significantly higher mental workload and higher frustration in the multitasking condition. It is worth noting that the variability in reaction times between users was also much higher in the multitasking condition. Indeed, the performance of a BCI is tightly related to the subjective mental workload experienced by the users (Felton et al., 2012), the higher the less the BCI performance would be. While the task difficulty was the same for all subjects, the subjective workloads experienced were different as it depends also on the skills, fatigue, etc. of the subjects. Nevertheless, the implemented rBCI demonstrate sufficient efficiency and responsiveness to be operated, even while flying and with high workload which was the aim.

Beside that, the pBCI findings also seemed to indicate the soundness of VEP to probe the level of attention to a monitoring

task. One of the main advantage of this approach is that the same calibration, lasting only 40 s, was used to train the rBCI and the pBCI. To the best of our knowledge, this is the first online demonstration that flickering stimuli could be used for pBCI purpose. The behavioral results showed that our pilots missed a total of 44 out of 203 collisions. The pBCI provided assistance to the pilots by simulating safety maneuvers with an acceptable rate of false negatives. We believe that this hybrid approach provides flexibility since the expertise of the pilot is kept at the center of the design, while providing a safety net in case the pilot's attentional resources are engaged on other aircraft operations. We consider it as an improvement compared to automatically activating the anti-collision safety whenever a collision is coming. In some cases, the pilot could have paid attention to this incoming danger but determined that the anti-collision safety was not necessary. In our scenario, the anti-collision safety was triggered only if the pilot deliberately chose to do it or if he or she was not paying attention. However, it is worthy to note that such adaptive automation could cause some drawbacks such as over-reliance on fallback mechanisms.

Despite these promising results it appeared that in eight cases out of 150, the pBCI did not detect pilot's attentional lapses

and failed to trigger the automatic maneuver (false positive). The occurrence of such failure could lead to critical scenarios in real-life situations. One has to keep in mind that we used a fixed empirical threshold set to 0.1 for all participants to infer the attentional state and trigger the pBCI. This fixed threshold, while proving to be efficient overall may not be optimal for each individual. A possible solution is to define an individualized threshold to obtain an optimal ratio between false positive and true negative. Interestingly enough, the findings disclosed that in nine instances out of 150 events, the pBCI classified that the participants detected the collision whereas the participants were not glancing at the radar as attested by the eye tracker (false negative). However, during the debriefing, the participants declared that they actually spotted the collision *via* peripheral vision. Such situation is possible since peripheral vision, *via* the rods, is highly sensitive to motion and flickering objects such as the VEP stimuli that were used in this experiment. For instance, some authors demonstrated the potential of using concurrent presentation of VEPs-based stimuli to assess processes outside of the focus of spatial attention (see for reviews Vialatte et al., 2010; Norcia et al., 2015). Future work should investigate this hypothesis.

Following on these promising results, this work calls for refinement through an actual implementation of the dBCI in the wild, i.e., under operational conditions. For instance and from an operating time point of view, it is blatant that using one's hands is still faster than the rBCI to interact with the cockpit. One solution is to provide hybrid interaction so that the pilots can choose to use either the BCI or physical modalities depending on the flight phase and time pressure. One could imagine that the pilot would interact through the BCI when the autopilot is engaged, so to increase his comfort and availability, and manually during more dynamic phases of the flights (i.e., maneuvers), when full commitment is required. In the present study the eye-tracking data were used as to provide a ground truth to assess both passive and reactive BCI performances in *post-hoc* analyses. The gaze data could also have been leveraged as a complementary source of spatial and temporal information to improve BCI speed and accuracy. Indeed, the eye-tracking data could provide contextual information, as to which area of the environment the user focuses attention. This contextual information (regions of interest in eye-tracking terminology), would lead to the activation of only a subset of the VEP stimuli based on the localization of user's attention (Lin et al., 2019). This approach would allow to artificially increase the number of classes while using a constant number of distinct VEPs therefore reducing the complexity of the classification problem (Stawicki et al., 2017). This lower number of distinct VEP also implies to acquire less calibration data compared to traditional paradigms in which each class is represented by a distinct VEP. Moreover, by triggering stimuli presentation, the eye-tracking data would provide the precise onset time of the stimuli thus giving valuable information for asynchronous BCI allowing to compute classification only when necessary and optimize computing power and time requirements. Additionally, gaze contingent rBCI would reduce the bottom-up influences of the visual stimuli on the user attentional resources. Indeed, the high contrast nature of stimuli

commonly used in VEP-based paradigms may distract attentional resources away from the primary task (Zhao et al., 2018). From an user experience perspective, the reduction in the number of VEP stimuli presented at the same time may improve visual comfort. Eventually, visual fixations on the radar area may be used as a two-step certification process to validate the VEP-based pBCI decision. Similarly for the rBCI, visual fixations within VEP stimuli area could be used to confirm the intention of an user to interact with a command. Overall eye-tracking information concurrent to VEP-based BCI classification outputs may be used to further improve classification performance and reduce the rate of false positives. This latter point is particularly important in the context of translating the proposed dual BCI system to real cockpit day-to-day flight operations as meeting high standards of aviation certification criteria is particularly challenging ( $10^{-3}$  allowable failure probability). In the context of aviation, any undesired activation of a command could jeopardize flight safety.

To conclude, we believe that the concept of dBCI opens promising prospects to improve human machine symbiosis for neuroergonomics applications in many domains such as transportation, industrial workplaces, medical care but also for disabled people. We have developed a proof of concept that relies on the code-VEP based stimuli and classification tools provided by the NextMind company. However, this approach is limited as it is a closed system. The EEG data streams are not accessible and the processing and classifications algorithms are not provided by the manufacturer. It is thus not possible to assess data quality or any data loss related issue. However, we hope that this study should encourage the development of open-source c-VEP code for the scientific community. Alternatively, other types of stimuli and classification procedures could be explored. For instance, the decoding of user's expectation (Zander et al., 2016) represent an interesting alternative since it does not require to present additional stimuli in the user interface. Combining together active and reactive tasks and the use of hybrid EEG and functional near infrared spectroscopy based BCI could maximize the number of commands (Hong and Khan, 2017) provided by a BCI. Regarding the pBCI, the use of more traditional features (e.g., changes in the well defined band of power for EEG) or more advanced ones like brain connectivity could be considered to target specific degraded mental states (cognitive fatigue, failure of auditory attention) so as to trigger the most appropriate neuro-adaptive solutions (Dehais et al., 2020b). Indeed, several solutions could be designed to dynamically optimize human-machine teaming by (1) adapting the user interface using notifications to alert of impeding hazards, (2) adapting the task and the level of automation to maintain the performance efficiency of the operators, and (3) "neuro-adapting" the end-users to warn them of their mental state and stimulate them to augment performance (e.g., neurofeedback). Eventually, some further work should be conducted to assess the effect of training with such system and stimuli, as few participants had a previous experience interacting with a BCI. It is generally reported that regular use of neurotechnology mitigates BCI illiteracy, improves classification accuracy and reduces reaction time (Blankertz et al., 2009). Also, future experiments could include a baseline condition without BCI use, to assess the effect

on pilots performance of such neurotechnology. We truthfully hope that this study will foster research efforts to improve the concept of dual BCI for safer, seamless, and efficient human-human and human(s)-machine(s) interactions.

## DATA AVAILABILITY STATEMENT

The datasets presented in this article are not readily available because, due to hardware limitation only eye tracking and subjective data are available. Requests to access the datasets should be directed to [frederic.dehais@isae.fr](mailto:frederic.dehais@isae.fr).

## ETHICS STATEMENT

The studies involving human participants were reviewed and approved by Comité d'Ethique de l'Université Fédérale de Toulouse (approval number 2020-334). The patients/participants provided their written informed consent to participate in this study.

## AUTHOR CONTRIBUTIONS

FD contributed to the conception and the design of experimental paradigm. FD, SL, and T-VN recorded the data. FD, T-VN, SL, and LD performed part of the analyses. SV, PL, GF,

and JT implemented the experimental set-up in the flight simulator. FD, SL, and LD wrote the manuscript. All authors revised the manuscript, read, and approved the submitted version.

## FUNDING

This research was funded by the Agence Innovation Défense of the Direction Générale de l'Armement (Neurosynchrone project).

## ACKNOWLEDGMENTS

The authors wish to sincerely thank all the pilots who participated in the experiment. The authors would also like to acknowledge the Artificial and Natural Intelligence Toulouse Institute (ANITI) and the Axa Research fund Neuroergonomics chair for flight safety for currently funding FD.

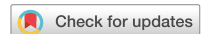
## SUPPLEMENTARY MATERIAL

The Supplementary Material for this article can be found online at: <https://www.frontiersin.org/articles/10.3389/fnrgo.2022.824780/full#supplementary-material>

## REFERENCES

- Aricó, P., Borghini, G., Di Flumeri, G., Colosimo, A., Bonelli, S., GOLFETTI, A., et al. (2016). Adaptive automation triggered by EEG-based mental workload index: a passive brain-computer interface application in realistic air traffic control environment. *Front. Hum. Neurosci.* 10:539. doi: 10.3389/fnhum.2016.00539
- Behrend, J., and Dehais, F. (2020). How role assignment impacts decision-making in high-risk environments: evidence from eye-tracking in aviation. *Saf. Sci.* 127:104738. doi: 10.1016/j.ssci.2020.104738
- Blankertz, B., Sanelli, C., Halder, S., Hammer, E., Kübler, A., Müller, K.-R., et al. (2009). Predicting BCI performance to study BCI illiteracy. *BMC Neurosci.* 10(Suppl. 1):P84. doi: 10.1186/1471-2202-10-S1-P84
- Borghini, G., Astolfi, L., Vecchiato, G., Mattia, D., and Babiloni, F. (2014). Measuring neurophysiological signals in aircraft pilots and car drivers for the assessment of mental workload, fatigue and drowsiness. *Neurosci. Biobehav. Rev.* 44, 58–75. doi: 10.1016/j.neubiorev.2012.10.003
- Brouwer, A.-M. (2021). Challenges and opportunities in consumer neuroergonomics. *Front. Neuroergon.* 2:3. doi: 10.3389/fnrgo.2021.606646
- Brouwer, A.-M., Hogervorst, M. A., Van Erp, J. B., Heffelaar, T., Zimmerman, P. H., and Oostenveld, R. (2012). Estimating workload using EEG spectral power and ERPs in the n-back task. *J. Neural Eng.* 9:045008. doi: 10.1088/1741-2560/9/4/045008
- Carelli, L., Solca, F., Faini, A., Meriggi, P., Sangalli, D., Cipresso, P., et al. (2017). Brain-computer interface for clinical purposes: cognitive assessment and rehabilitation. *BioMed Res. Int.* 2017:1695290. doi: 10.1155/2017/1695290
- Chevallier, S., Kalunga, E. K., Barthélémy, Q., and Monacelli, E. (2021). Review of riemannian distances and divergences applied to SSVEP-based BCI. *Neuroinformatics* 19, 93–106. doi: 10.1007/s12021-020-09473-9
- Clerc, M., Bougrain, L., and Lotte, F. (2016). *Brain-Computer Interfaces* 1. Hoboken, NJ: Wiley-ISTE. doi: 10.1002/9781119144977
- Dehais, F., Duprés, A., Blum, S., Drougard, N., Scannella, S., Roy, R. N., et al. (2019a). Monitoring pilot's mental workload using ERPs and spectral power with a six-dry-electrode EEG system in real flight conditions. *Sensors* 19:1324. doi: 10.3390/s19061324
- Dehais, F., Duprés, A., Di Flumeri, G., Verdiere, K., Borghini, G., Babiloni, F., et al. (2018). “Monitoring pilot's cognitive fatigue with engagement features in simulated and actual flight conditions using an hybrid fNIRS-EEG passive BCI,” in *2018 IEEE International Conference on Systems, Man, and Cybernetics (SMC)* (Miyazaki), 544–549. doi: 10.1109/SMC.2018.00102
- Dehais, F., Karwowski, W., and Ayaz, H. (2020a). Brain at work and in everyday life as the next frontier: grand field challenges for neuroergonomics. *Front. Neuroergon.* 1:583733. doi: 10.3389/fnrgo.2020.583733
- Dehais, F., Lafont, A., Roy, R., and Fairclough, S. (2020b). A neuroergonomics approach to mental workload, engagement and human performance. *Front. Neurosci.* 14:268. doi: 10.3389/fnins.2020.00268
- Dehais, F., Rida, I., Roy, R. N., Iversen, J., Mullen, T., and Callan, D. (2019b). “A PBCI to predict attentional error before it happens in real flight conditions,” in *2019 IEEE International Conference on Systems, Man and Cybernetics (SMC)* (Bari), 4155–4160. doi: 10.1109/SMC.2019.8914010
- Dehais, F., Roy, R. N., and Scannella, S. (2019c). Inattentional deafness to auditory alarms: inter-individual differences, electrophysiological signature and single trial classification. *Behav. Brain Res.* 360, 51–59. doi: 10.1016/j.bbr.2018.11.045
- Ewing, K. C., Fairclough, S. H., and Gilleade, K. (2016). Evaluation of an adaptive game that uses EEG measures validated during the design process as inputs to a biocybernetic loop. *Front. Hum. Neurosci.* 10:223. doi: 10.3389/fnhum.2016.00223
- Fairclough, S. H., and Lotte, F. (2020). Grand challenges in neurotechnology and system neuroergonomics. *Front. Neuroergon.* 1:2. doi: 10.3389/fnrgo.2020.602504
- Felton, E., Williams, J., Vanderheiden, G., and Radwin, R. (2012). Mental workload during brain-computer interface training. *Ergonomics* 55, 526–537. doi: 10.1080/00140139.2012.662526
- Fricke, T., Zander, T., Gramann, K., and Holzapfel, F. (2014). “First pilot-in-the-loop simulator experiments on brain control of horizontal aircraft motion,” in *Deutscher Luft-und Raumfahrtkongress* (Bonn).

- Gateau, T., Ayaz, H., and Dehais, F. (2018). *In silico* vs. over the clouds: on-the-fly mental state estimation of aircraft pilots, using a functional near infrared spectroscopy based passive-BCI. *Front. Hum. Neurosci.* 12:187. doi: 10.3389/fnhum.2018.00187
- Gembler, F., Benda, M., Rezeika, A., Stawicki, P., and Volosyak, I. (2020). Asynchronous c-VEP communication tools-efficiency comparison of low-target, multi-target and dictionary-assisted BCI spellers. *Sci. Rep.* 10:17064. doi: 10.1038/s41598-020-74143-4
- Gramann, K., McKendrick, R., Baldwin, C., Roy, R. N., Jeunet, C., Mehta, R. K., et al. (2021). Grand field challenges for cognitive neuroergonomics in the coming decade. *Front. Neuroergon.* 2:6. doi: 10.3389/fnrgo.2021.643969
- Hancock, P. A., and Szalma, J. L. (2008). "Stress and neuroergonomics," in *Neuroergonomics: The Brain at Work*, eds R. Parasuraman and M. Rizzo (New York, NY: Oxford University), 195–206.
- Hong, K.-S., and Khan, M. J. (2017). Hybrid brain-computer interface techniques for improved classification accuracy and increased number of commands: a review. *Front. Neurorobot.* 11:35. doi: 10.3389/fnbot.2017.00035
- Hughes, C. L., Herrera, A., Gaunt, R., and Collinger, J. (2020). "Bidirectional brain-computer interfaces," in *Handbook of Clinical Neurology*, eds N. F. Ramsey and J. R. Milla (Elsevier), 163–181. doi: 10.1016/B978-0-444-63934-9.00013-5
- Kahneman, D. (1973). *Attention and Effort*, Vol. 88. Englewood Cliffs, NJ: University of Illinois Press.
- Kalunga, E. K., Chevallier, S., Barthélémy, Q., Djouani, K., Monacelli, E., and Hamam, Y. (2016). Online SSVEP-based BCI using Riemannian geometry. *Neurocomputing* 191, 55–68. doi: 10.1016/j.neucom.2016.01.007
- Klaproth, O. W., Halbrügge, M., Krol, L. R., Vernaleken, C., Zander, T. O., and Russwinkel, N. (2020). A neuroadaptive cognitive model for dealing with uncertainty in tracing pilots' cognitive state. *Top. Cogn. Sci.* 12, 1012–1029. doi: 10.1111/tops.12515
- Lin, X., Chen, Z., Xu, K., and Zhang, S. (2019). "Development of a high-speed mental spelling system combining eye tracking and SSVEP-based BCI with high scalability," in *Proceedings of the Annual International Conference of the IEEE Engineering in Medicine and Biology Society, EMBS* (Berlin), 6318–6322. doi: 10.1109/EMBC.2019.8857408
- Lotte, F., Bougrain, L., Cichocki, A., Clerc, M., Congedo, M., Rakotomamonjy, A., et al. (2018). A review of classification algorithms for EEG-based brain-computer interfaces: a 10 year update. *J. Neural Eng.* 15:031005. doi: 10.1088/1741-2552/aab2f2
- Lotte, F., and Roy, R. N. (2019). "Chapter 7: Brain-computer interface contributions to neuroergonomics," in *Neuroergonomics*, eds H. Ayaz and F. Dehais (Amsterdam: Academic Press), 43–48. doi: 10.1016/B978-0-12-811926-6.00007-5
- Maksimenko, V. A., Hramov, A. E., Frolov, N. S., Lüttjohann, A., Nedai佐佐, V. O., Grubov, V. V., et al. (2018). Increasing human performance by sharing cognitive load using brain-to-brain interface. *Front. Neurosci.* 12:949. doi: 10.3389/fnins.2018.00949
- Matthews, G., Reinerman-Jones, L., Abich, J. IV., and Kustubayeva, A. (2017). Metrics for individual differences in EEG response to cognitive workload: optimizing performance prediction. *Pers. Individ. Differ.* 118, 22–28. doi: 10.1016/j.paid.2017.03.002
- Mumaw, R., Haworth, L., and Feary, M. (2019). *The Role of Alerting System Failures in Loss of Control Accidents Cast SE-210 Output 2 Report 3 of 6*. NASA Technical Memorandum - SeaWiFS Technical Report Series. NASA AMES.
- Nagel, S., and Spüler, M. (2019). World's fastest brain-computer interface: combining EEG2CODE with deep learning. *PLoS ONE* 14:e221909. doi: 10.1371/journal.pone.0221909
- Nakanishi, M., Wang, Y., Chen, X., Wang, Y. T., Gao, X., and Jung, T. P. (2018). Enhancing detection of SSVEPs for a high-speed brain speller using task-related component analysis. *IEEE Trans. Biomed. Eng.* 65, 104–112. doi: 10.1109/TBME.2017.2694818
- Norcia, A. M., Appelbaum, L. G., Ales, J. M., Cottereau, B. R., and Rossion, B. (2015). The steady-state visual evoked potential in vision research: a review. *J. Vis.* 15, 4–44. doi: 10.1167/15.6.4
- Nourmohammadi, A., Jafari, M., and Zander, T. O. (2018). A survey on unmanned aerial vehicle remote control using brain-computer interface. *IEEE Trans. Hum. Mach. Syst.* 48, 337–348. doi: 10.1109/THMS.2018.2830647
- Prinzel, L. J., Freeman, F. G., Scerbo, M. W., Mikulka, P. J., and Pope, A. T. (2000). A closed-loop system for examining psychophysiological measures for adaptive task allocation. *Int. J. Aviat. Psychol.* 10, 393–410. doi: 10.1207/S15327108IJAP1004\_6
- Rodriguez-Bermudez, G., Lopez-Belchi, A., and Girault, A. (2019). Testing brain-computer interfaces with airplane pilots under new motor imagery tasks. *Int. J. Comput. Intell. Syst.* 12, 937–946. doi: 10.2991/ijcis.d.190806.001
- Roy, R. N., Bonnet, S., Charbonnier, S., and Campagne, A. (2016). Efficient workload classification based on ignored auditory probes: a proof of concept. *Front. Hum. Neurosci.* 10:519. doi: 10.3389/fnhum.2016.00519
- Scholl, C. A., Chi, Y. M., Elconin, M., Gray, W. R., Chevillet, M. A., and Pohlmeier, E. A. (2016). "Classification of pilot-induced oscillations during in-flight piloting exercises using dry EEG sensor recordings," in *2016 38th Annual International Conference of the IEEE Engineering in Medicine and Biology Society (EMBC)* (Orlando, FL), 4467–4470. doi: 10.1109/EMBC.2016.7591719
- Shirzhiyan, Z., Keihani, A., Farahi, M., Shamsi, E., GolMohammadi, M., Mahnam, A., et al. (2019). Introducing chaotic codes for the modulation of code modulated visual evoked potentials (c-VEP) in normal adults for visual fatigue reduction. *PLoS ONE* 14:e213197. doi: 10.1371/journal.pone.0213197
- Stawicki, P., Gembler, F., Rezeika, A., and Volosyak, I. (2017). A novel hybrid mental spelling application based on eye tracking and SSVEP-based BCI. *Brain Sci.* 7:35. doi: 10.3390/brainsci7040035
- Vecchiato, G., Borghini, G., Aricó, P., Graziani, I., Maglione, A. G., Cherubino, P., et al. (2016). Investigation of the effect of EEG-BCI on the simultaneous execution of flight simulation and attentional tasks. *Med. Biol. Eng. Comput.* 54, 1503–1513. doi: 10.1007/s11517-015-1420-6
- Vialatte, F.-B., Maurice, M., Dauwels, J., and Cichocki, A. (2010). Steady-state visually evoked potentials: focus on essential paradigms and future perspectives. *Prog. Neurobiol.* 90, 418–438. doi: 10.1016/j.pneurobio.2009.11.005
- Wickens, C., and Dehais, F. (2019). *Expertise in Aviation*. Oxford: Oxford University Press. doi: 10.1093/oxfordhb/9780198795872.013.29
- Wickens, C. D. (2008). Multiple resources and mental workload. *Hum. Factors* 50, 449–455. doi: 10.1518/001872008X288394
- Wickens, C. D., and Alexander, A. L. (2009). Attentional tunneling and task management in synthetic vision displays. *Int. J. Aviat. Psychol.* 19, 182–199. doi: 10.1080/10508410902766549
- Zander, T. O., and Kothe, C. (2011). Towards passive brain-computer interfaces: applying brain-computer interface technology to human-machine systems in general. *J. Neural Eng.* 8:025005. doi: 10.1088/1741-2560/8/2/025005
- Zander, T. O., Krol, L. R., Birbaumer, N. P., and Gramann, K. (2016). Neuroadaptive technology enables implicit cursor control based on medial prefrontal cortex activity. *Proc. Natl. Acad. Sci. U.S.A.* 113, 14898–14903. doi: 10.1073/pnas.1605155114
- Zhao, Y., Tang, J., Cao, Y., Jiao, X., Xu, M., Zhou, P., Ming, D., et al. (2018). Effects of distracting task with different mental workload on steady-state visual evoked potential based brain computer interfaces - an offline study. *Front. Neurosci.* 12:79. doi: 10.3389/fnins.2018.00079
- Zhu, D., Bieger, J., Garcia Molina, G., and Aarts, R. M. (2010). A survey of stimulation methods used in SSVEP-based BCIs. *Comput. Intell. Neurosci.* 2010:702357. doi: 10.1155/2010/702357
- Conflict of Interest:** The authors declare that the research was conducted in the absence of any commercial or financial relationships that could be construed as a potential conflict of interest.
- Publisher's Note:** All claims expressed in this article are solely those of the authors and do not necessarily represent those of their affiliated organizations, or those of the publisher, the editors and the reviewers. Any product that may be evaluated in this article, or claim that may be made by its manufacturer, is not guaranteed or endorsed by the publisher.
- Copyright © 2022 Dehais, Ladouce, Darmet, Nong, Ferraro, Torre Tresols, Velut and Labedan. This is an open-access article distributed under the terms of the Creative Commons Attribution License (CC BY). The use, distribution or reproduction in other forums is permitted, provided the original author(s) and the copyright owner(s) are credited and that the original publication in this journal is cited, in accordance with accepted academic practice. No use, distribution or reproduction is permitted which does not comply with these terms.



OPEN

# Improving user experience of SSVEP BCI through low amplitude depth and high frequency stimuli design

S. Ladouce<sup>1</sup>✉, L. Darmet<sup>1</sup>, J. J. Torre Tresols<sup>1</sup>, S. Velut<sup>1</sup>, G. Ferraro<sup>1</sup> & F. Dehais<sup>1,2</sup>

Steady-States Visually Evoked Potentials (SSVEP) refer to the sustained rhythmic activity observed in surface electroencephalography (EEG) in response to the presentation of repetitive visual stimuli (RVS). Due to their robustness and rapid onset, SSVEP have been widely used in Brain Computer Interfaces (BCI). However, typical SSVEP stimuli are straining to the eyes and present risks of triggering epileptic seizures. Reducing visual stimuli contrast or extending their frequency range both appear as relevant solutions to address these issues. It however remains sparsely documented how BCI performance is impacted by these features and to which extent user experience can be improved. We conducted two studies to systematically characterize the effects of frequency and amplitude depth reduction on SSVEP response. The results revealed that although high frequency stimuli improve visual comfort, their classification performance were not competitive enough to design a reliable/responsive BCI. Importantly, we found that the amplitude depth reduction of low frequency RVS is an effective solution to improve user experience while maintaining high classification performance. These findings were further validated by an online T9 SSVEP-BCI in which stimuli with 40% amplitude depth reduction achieved comparable results (>90% accuracy) to full amplitude stimuli while significantly improving user experience.

The Steady-States Visually Evoked Potentials (SSVEP) characterize neural responses to the presentation of periodic visual stimuli (RVS). The light information, either from Light Emitting Diodes (LED) arrays or rendered on a computer screen<sup>1</sup>, stimulates photoreceptor cells (cones and rods) in the retina that eventually reaches retinal ganglion cells. These cells are neurons whose activation triggers an action potentials cascade that propagates through the optic nerve to carry visual information to cortical areas. The sustained rhythmic entrainment of neuronal populations in the visual cortex to the attended RVS frequency can be recorded with surface electro-encephalography (EEG). The distinctive properties of the RVS are reflected by the spectral components of the recorded EEG signal. Such effect has been widely taken advantage of to implement reactive brain computer interface (BCI). Reactive BCI are defined as the decoding of the EEG signal elicited by the presentation of a stimulus that corresponds to a specific output command. In practice, a prototypical implementation of SSVEP-based reactive BCI consists in the simultaneous presentation of several RVS varying in frequency. By focusing one's attention to a specific stimulus, a SSVEP response is elicited and then decoded through the extraction of spatial and temporal features of the EEG signal to be fed to classification algorithms<sup>2</sup>. The classification of a SSVEP response triggers the associated command output (e.g., key press for a speller).

Historically, stimuli were mainly consisting in *on/off* flickering LED. Recent methods use computer screen to present flickering or pattern-reversal images (typically following a sinusoidal or square wave)<sup>3</sup>. The design of RVS for SSVEP-based BCI application has mainly focused on maximising the Signal-to-Noise Ratio (SNR) of the SSVEP response to achieve high classification performance. Notably, increasing amplitude depth between stimuli states (i.e. contrast)<sup>4</sup>, increasing stimuli luminance<sup>5</sup> or reducing user's distance from SSVEP stimulator<sup>6</sup> have proven to be successful approaches to maximise SNR. These methods are however detrimental to the user experience as they make the RVS more visually intrusive<sup>7</sup>. Over prolonged exposition, RVS may cause eye strain leading to visual fatigue but also reduction in task performance and headaches<sup>3</sup>. It should also be noted that SSVEP responses have been mainly studied within the 4 to 20Hz. This is due to a combination of hardware limitations (common monitors were limited to a 60 Hz refresh rate) and the 1/f law characterizing power

<sup>1</sup>Human Factors and Neuroergonomics, ISAE-SUPAERO, 31000 Toulouse, France. <sup>2</sup>Biomedical Engineering, Drexel University, Philadelphia, PA, USA. ✉email: simon.ladouce@isae-supaero.fr

distribution over the EEG spectrum. The maximal SNR for SSVEP responses has been typically observed around 15 Hz<sup>8,9</sup> leading to the adoption of low frequencies stimuli for the design of SSVEP BCI. Concerns about health risks have however been raised as the presentation of high luminance RVS in the 8–20 Hz range may trigger epileptic seizures in photosensitive individuals<sup>10</sup>. These issues are of critical importance as they not only limit the population that can effectively use SSVEP BCI but they also imply serious health hazards for individuals with undiagnosed photosensitive epilepsy.

A first solution to address the aforementioned issues would be to use frequencies above 20 Hz in order to make RVS safer and more comfortable to the users. Previous research investigating high frequency SSVEP responses (> 20 Hz) have mainly used LEDs displays of intense luminance. Herrmann<sup>11</sup> reported SSVEP responses up to 100 Hz with a 1/f trend characterizing the magnitude of the responses<sup>12</sup> and Muller et al.<sup>13</sup> demonstrated the feasibility of asynchronous BCI control of a cursor using high frequency RVS (4 LEDs placed around a screen) flickering at 37 to 40 Hz. Chabuda et al.<sup>14</sup> used 30 to 39 Hz RVS in a 8-class online BCI speller, reporting an average classification accuracy of 96%<sup>15</sup> disclosed online classification accuracy for high frequency ranges (98.4% for 30–35 Hz, 99% for 35–40 Hz and 95.2% for 40–45 Hz) in a 5 class problem with LED used as SSVEP generators. However, these classification performance were only attained using long epoch length (up to 10 s) which severely limits the responsiveness of a BCI. More recent studies have applied offline analysis on 2 s epochs and Liang et al.<sup>16</sup> reported 91% classification accuracy on a 40-class BCI paradigm using 30 to 36Hz RVS whereas Yue et al.<sup>17</sup> reached 87% with only 1 s epoch length using 31 to 40 Hz. It is important to note that most of these studies used high luminance LED arrays placed relatively close to the participants' eyes. This stimulation method to elicit SSVEP is arguably not suited for a daily usage, especially over prolonged use.

A second solution to improve user experience and visual comfort would be to reduce the contrast and intensity of RVS by lowering their amplitude depth. Stimulus amplitude depth refers to the contrast difference between the two antagonist states of a RVS. The mean luminance intensity is also reduced as the maximal luminance reached is lowered. In most SSVEP-based BCI implementation, the amplitude depth used is maximal. This practice is in line with findings from research on the visual system highlighting the sensitivity of primary visual cortical areas (V1) to high contrast stimuli<sup>18</sup> and larger foveal magnification<sup>19</sup> in response to high luminance visual information. In a recent study, Chang et al.<sup>20</sup> have investigated the relevance of Amplitude Modulation (AM) for RVS to reduce eye fatigue. The AM approach consists in the modulation of the amplitude of the flickering signal by another oscillating signal of higher frequency (the carrier) over time. The authors concluded that AM, although leading to a reduction of stimuli intensity on average, was only merely perceptible to the users and did not lead to a clear improvement of visual comfort. It is important to distinguish the Amplitude Modulation approach from RVS amplitude depth reduction. Moreover, AM modulation implies an increase in the spectral complexity of the SSVEP signal, which decreases classification performance. More recently Lingelbach et al.<sup>21</sup>, reported SSVEP responses below an user-defined contrast perceptual threshold. The condition in which the RVS were below the perceptual threshold was rated as more visually comfortable by the participants. The RVS were not presented simultaneously but individually, thus relevance for BCI application and classification performance of stimuli below perceptual threshold remain to be assessed. In another study<sup>22</sup>, the authors demonstrated that a 90% reduction of the maximal amplitude depth significantly improved visual comfort. The classification accuracy, although diminished in comparison to full amplitude depth RVS, was still around 80% for a 4-class problem (using a 3s window length). These studies sparked interest in amplitude depth reduction as a mean to improve RVS visual comfort and overall user experience during SSVEP-based BCI control.

Taken together, these findings indicate that increasing the frequency and reducing the amplitude depth of RVS are both promising approaches to make SSVEP-based BCI more comfortable and safer to use. Previous studies have however revealed that such approaches may reduce the SSVEP signal strength and therefore classification performance. Consequently, a compromise between user experience and classification performance need to be established. For this purpose we present a series of three experiments that manipulate RVS frequency and amplitude depth in a systematic manner:

- The first experiment aimed to evaluate user experience and characterize SSVEP responses elicited across 24 frequencies ranging from 8 to 60Hz (see Fig. 7);
- The second experiment aimed to investigate the effect of amplitude depth reduction (100, 50, 40, 30, 20 and 10%) on low and high frequency SSVEP responses and user experience (see Fig. 7);
- The third experiment consisted in bench-marking an online T9 BCI whose design was based on previous experiments findings. Three different RVS designs (low frequency and full amplitude vs low frequency and low amplitude depth reduction vs high frequency and subtle amplitude depth reduction).

The main ambition of the present research was to improve SSVEP-based BCI user experience. As such, subjective assessment of RVS visual comfort played a pivotal role in the decisions made regarding experimental designs across the three experiments. In addition to the measures of user experience (assessing the intrusiveness, visual comfort, and fatigue related to the presentation of RVS), SSVEP SNR and the performance of the state-of-the art classification algorithm were contrasted across the different designs.

## Results

**Experiment 1: effect of RVS frequency.** This first experiment systematically compared the classification performance, subjective visual comfort and SSVEP SNR for RVS of different frequencies ranging from 8 to 60 Hz, with a step of 2 Hz.

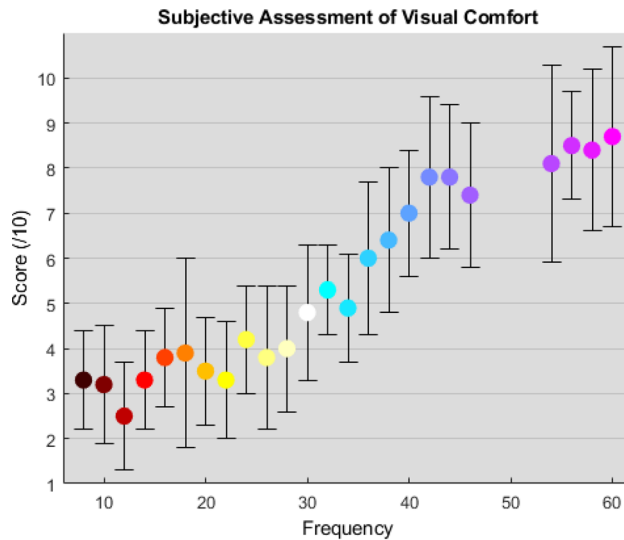


**Figure 1.** Experiment 1: relationship between RVS frequency (ranging from 8 to 60 Hz with a step increase of 2 Hz at the exclusion of 48 to 52 Hz) and the subjective visual comfort score.

*User experience.* The RVS frequency had a main effect on the subjective visual comfort score [ $F(23,264) = 22.369, p < .001, n^2 = 0.661$ ]. There was a strong positive relationship between RVS frequency and subjective assessment of visual comfort ( $r(288) = .781, p < .001$ ). As illustrated in Fig. 1, a substantial difference in subjective experience was observed across the range of frequencies. The highest RVS frequency (60 Hz) are deemed much more comfortable (mean score = 8.6, SD = 1.9) than the lowest RVS frequency (mean score = 3.3, SD = 1). The subjective rating of fatigue [ $F(23,264) = 19.035, p < .001, n^2 = 0.624$ ] and intrusiveness [ $F(23,264) = 11.506, p < .001, n^2 = 0.501$ ] followed a similar trend with high frequency stimuli rated as less tiring and less intrusive than lower frequency RVS.

*Critical flicker-fusion frequency.* The mean flicker-fusion frequency threshold, referring to the frequency above which the RVS is not perceived as flickering, was found to be at 67.9 Hz on average ( $SD = 2$ ) which is in line with previous psycho-physics findings<sup>23</sup>. More details can be found in the Supplementary Information.

*SSVEP signal-to-noise ratio.* An ANOVA revealed a main effect of the RVS frequency on SSVEP SNR [ $F(23,264) = 8.607, p < .001, n^2 = 0.429$ ]. The SNR was negatively correlated to stimulus frequency ( $r(288) = -.692, p < .001$ ) as can be observed in Fig. 2.

*Classification performance.* The task related component analysis (TRCA)<sup>25</sup> classifier was applied to both low and high frequency data separately. Thus the classification was performed for each condition separately splitting the data into 12 classes for each condition. For the low frequencies range (from 8 to 30 Hz), we observe that the best classification performances were achieved between 10 and 15 Hz. This result is in line with previous reports from<sup>8,9</sup>. A steep decrease of around 20% in classification accuracy was noted between the optimal frequency 14 Hz and frequencies above 20 Hz. In regards to the higher frequency range (above 30 Hz) a plateau of around 70% classification accuracy was observed from 30 to 38 Hz. The breaking point was observed around 40 Hz, above which the classification performance severely declined. Additional details can be found in the confusion matrices included in the Supplementary Materials. These results are coherent with the SNR measures (see above), as SSVEP responses elicited by RVS above 40 Hz exhibited the lowest SNR values. It should be noted that this 40 Hz breaking point is far below the mean flicker fusion threshold measured at 67.9Hz. Although high frequency RVS elicited SSVEP responses, the classification performance is insufficient to ensure reliable BCI control. Furthermore, inter-subjects variability in classification accuracy increased significantly for frequencies above 36 Hz. It suggests that the highest RVS frequency that should be considered for an SSVEP-based BCI is 36 Hz.

**Experiment 2: effect of RVS amplitude depth reduction.** This experiment is intended to study the impact on relative comfort and performance of reduced depth amplitude stimuli, using both high and low frequencies.

*User experience.* Both the RVS frequency [ $F(7,77) = 40.88, p < .001, n^2 = 0.339$ ] and RVS amplitude depth [ $F(5,55) = 196.376, p < .001, n^2 = 0.389$ ] had a main effect on subjective assessment of RVS visual comfort. As shown in Fig. 3, the users rated the RVS more comfortable as their frequency increased [ $r(576) = .573, p < .001$ ] and their amplitude depth decreased [ $r(576) = .602, p < .001$ ]. The users reported that stimuli at higher frequencies induced less visual fatigue [ $r(576) = -.556, p < .001$ ] but also that lower amplitude depth RVS reduced

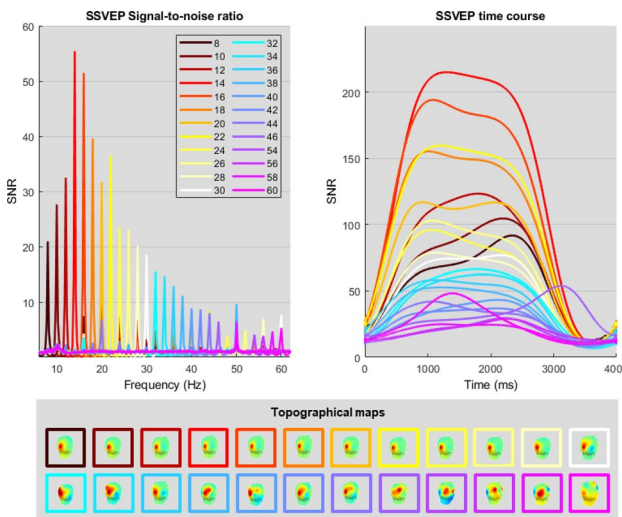


**Figure 2.** Experiment 1: rhythmic entrainment source separation (RESS)<sup>24</sup> analyses of SSVEP responses to RVS ranging from 8 to 60 Hz (step increase of 2 Hz, with the exclusion of line noise neighbouring frequencies 48, 50 and 52 Hz). Top left: power spectrum of the SSVEP signal-to-noise ratio (SNR). Top right: SSVEP response over the course of the 3 s RVS presentation. Bottom: topographical distribution of SSVEP responses to RVS.

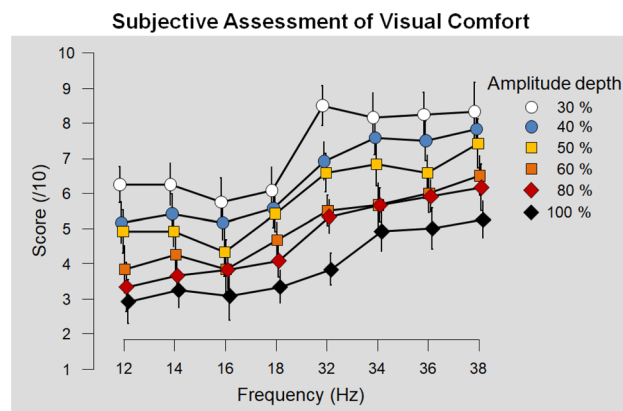


**Figure 3.** Experiment 2: subjective visual comfort score across RVS frequency ranges (low: 12, 14, 16, 18; high: 32, 34, 36, 38 Hz) for each RVS amplitude depth (30, 40, 50, 60, 80 and 100% of the maximal amplitude).

ocular fatigue [ $r(576) = .568$ ,  $p < .001$ ]. Regarding RVS intrusiveness, participants reported that RVS at higher frequency were less salient [ $r(576) = .560$ ,  $p < .001$ ] and that lower amplitude RVS were also deemed as less intrusive [ $r(576) = .528$ ,  $p < .001$ ].

**Contrast perceptual threshold.** The perception threshold of RVS following reduction of amplitude depth was assessed for each frequency individually using a staircase method (0.2 increments/decrements) for the definition of perceptual threshold. A repeated measures ANOVA with frequency (12, 14, 16, 18, 32, 34, 36, 38 Hz) as factor was performed on contrast perceptual threshold measures. The results reveal a main effect of frequency on the amplitude depth threshold at which the RVS were not perceived [ $F(7,77) = 28.918$ ,  $p < .001$ ,  $n^2 = 1$ ]. There was a strong positive correlation between RVS frequency and the amplitude depth at which the stimuli were not perceived anymore [ $r(96) = .97$ ,  $p < .001$ ]. While lower frequencies were still perceived at around 0.8% ( $SD = 0.026$ ) of the maximal amplitude depth, higher frequencies exhibited higher thresholds (around 3.1–4%,  $SD = 0.034$ ). Some more details can be found in the Supplementary Information.

**SSVEP signal-to-noise ratio.** A repeated measures  $6 \times 8$  ANOVA with amplitude depths (100, 80, 60, 50, 40, 30) and frequencies (12, 14, 16, 18, 32, 34, 36, 38 Hz) as factors was performed on RESS SNR measures. Both the amplitude depth [ $F(5,55) = 3.009$ ,  $p = .018$ ,  $n^2 = 0.016$ ] and RVS frequency [ $F(7,77) = 7.883$ ,  $p < .001$ ,  $n^2 = 0.335$ ] showed a significant effect on SSVEP SNR. There was however no significant interaction found between the two factors on SSVEP SNR [ $F(35,385) = 0.618$ ,  $p = .958$ ,  $n^2 = 0.007$ ]. A negative Pearson correlation between

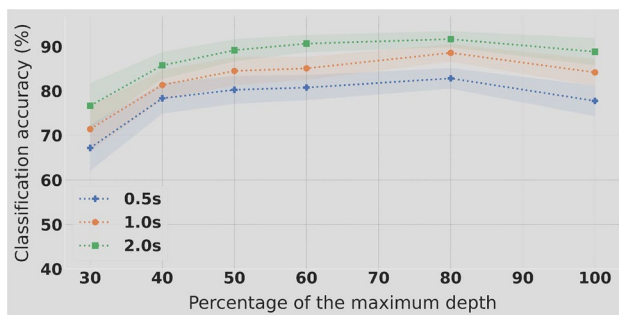


**Figure 4.** Experiment 2: classification accuracy in % using 4 classes (12, 14, 16 and 18 Hz) in function of different levels of amplitude stimulation depth and considering 3 epochs lengths.

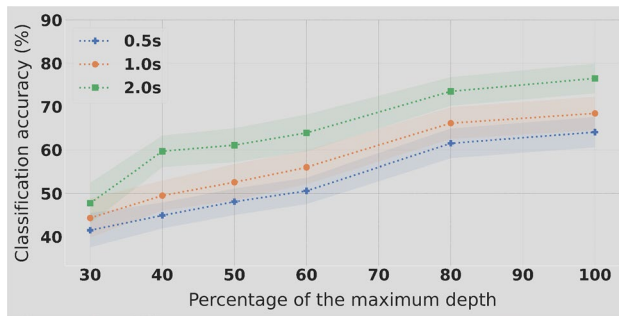


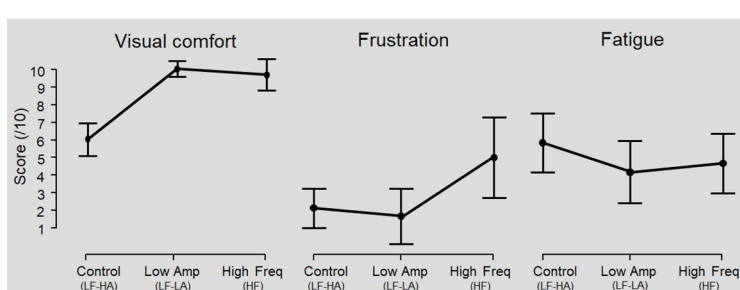
**Figure 5.** Experiment 2: classification accuracy in % using 4 classes (32, 34, 36 and 38 Hz) in function of different levels of amplitude stimulation depth and considering 3 epochs lengths.

SSVEP SNR and RVS frequency was observed [ $\text{rs}(576) = -.553, p < .001$ ]. A moderate linear relationship between SSVEP SNR and RVS amplitude depth was also found [ $\text{rs}(576) = .132, p < .01$ ]. In brief, post-hoc comparisons revealed that lower frequencies had significantly higher SNR than high frequencies (except 32 Hz).

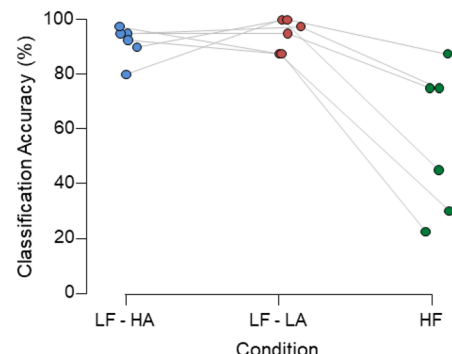
**Classification performance.** The TRCA classifier was used to tackle a 4 classes problem corresponding to four distinct RVS frequencies. The amplitude depth reduction for the lower frequencies, 12, 14, 16 and 18 Hz, had a significant impact on classification accuracy only for amplitude depth levels below 50%. As can be observed on Fig. 4, above this threshold the classification accuracy estimation is higher with lower variability across individuals. Below 50% of maximal amplitude depth, a significant drop in accuracy is observed. The dynamic is quite different for the higher frequencies (32, 34, 36 and 38 Hz). As depicted on Fig. 5, there is a linear trend between the increase of amplitude depth and the classification accuracy. The gain in performance is smaller between 90% and 100%. Even though a decrease in stimuli amplitude depth is providing a better user experience, it does not seem to be operable because of the low classification performance when significant reduction (more than 30%) is considered. Only a 90% reduction could be considered as the classification accuracy drop is moderated.

**Experiment 3: an online T9 experiment with improved comfort.** The latter experiment involved an online setting of PIN code typing through a T9 keyboard. Based on results of Experiment 1 and 2, we have considered a first condition using low frequencies stimuli (8–12 Hz) with 60% of the maximal amplitude depth, then high frequencies (28–32 Hz) stimuli with 90% of the maximal amplitude depth to finally be compared to the reference condition of low frequency (8–12 Hz) with full amplitude (100%).

**User experience.** The participants were surveyed about how visually comfortable the stimuli were, how tired they felt after completing calibration plus testing phase and how frustrating the testing phase was for each condition. A main effect was found on both visual comfort [ $F(2,10) = 53.2, p < 0.001, n^2 = 0.914$ ] and perceived frustration [ $F(2,10) = 7.287, p = 0.011, n^2 = 0.593$ ] whereas no main effect on the fatigue reported by the participants was found [ $F(2,10) = 1.65, p = 0.24, n^2 = 0.248$ ]. Low amplitude and high frequency stimuli were deemed as more visually comfortable than stimuli from the reference condition [reference—low amp:  $t(5) = 10.95, p < 0.001, d = 4.47, BF_{10} = 222.87$ ; reference—high freq:  $t(5) = 6.57, p = 0.001, d = 2.68, BF_{10} = 34.26$ ]. While the user experience during the testing phase of both low frequency conditions was rated as not frustrating (Low Frequencies High Amplitude: mean = 1.33, SD = 1.211; Low Frequencies Low Amplitude: mean = 0.833, SD = 1.169), the high frequency condition induced significantly more frustration (mean = 4.5, SD = 3.61) [high freq—control:  $t(5) = 2.78, p = 0.04, d = 1.13, BF_{10} = 2.5$ ; high freq—low amp:  $t(5) = 2.8, p = 0.038, d = 1.14, BF_{10} = 2.5$ ]. A positive linear relationship between frustration experienced and classification performance was



**(a)** Assessment of user experience of each BCI condition (control, low amplitude and high frequency). Participants were surveyed about three components (visual comfort, fatigue, frustration) using a visual analog scale (rating ranging from 1 to 10).



**(b)** Distribution of online classification accuracy for the Low Frequency - High Amplitude (LF - HA), Low Frequency - Low Amplitude (LF - LA) and High Frequency (HF) conditions across subjects.

**Figure 6.** Experiment 3: subjective and classification accuracy results for the different conditions of the online T9 BCI.

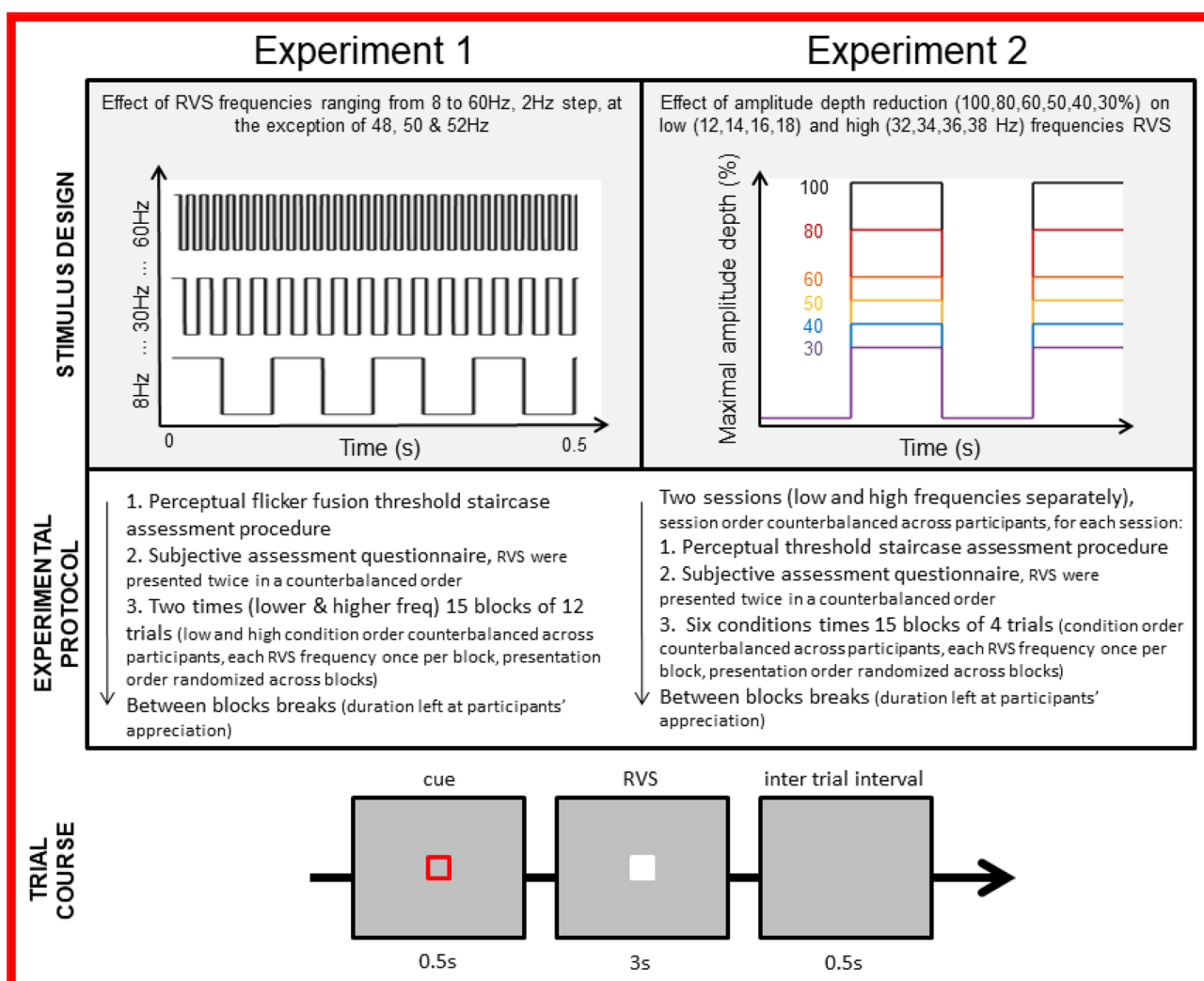


**Figure 7.** Experiments 1 and 2 : illustration of the repeated visual stimuli (RVS) design for each experiment (manipulating stimuli frequency and amplitude depth), experimental protocols descriptions and a diagram presenting trial course parameters used across both experiments.

found for both the low amplitude [ $r(5) = .84, p = .03$ ] and high frequency [ $r(5) = .93, p < .01$ ] conditions. From an user experience point of view, high frequency and low amplitude stimuli were preferred by the participants as they were perceived as more visually comfortable. The experience of high frequency BCI was however deemed frustrating due to its low classification performance.

**Classification accuracy.** The online accuracy obtained using TRCA classifier for the three conditions are summarized in Fig. 6b. The control condition (low frequencies and full amplitude) reached an accuracy of 91.7% ( $ITR = 35.9$  bpm). It is to be compared with the low amplitude low frequencies condition with 94.6% ( $ITR = 38.6$  bpm) and to the high frequencies conditions with mean performance of respectively with 55.8% ( $ITR = 13.0$  bpm). Thus, no significant difference in terms of classification accuracy was found between the low amplitude and the control condition [ $t(5) = .66, p = .53, d = .27, BF_{10} = .44$ ] while performance of high frequency RVS were significantly lower. Additionally, we have observed a high variability in the inter-subjects performance for the high frequencies stimuli, as depicted by the green dots dispersion in Fig. 6b. These performances are in line with Experiment 2 findings suggesting that the use of high frequencies ( $> 30$  Hz) implies higher variability in classification performance across subjects.

## Discussion

The overarching goal of this study was to inform the design of RVS improving the user experience of SSVEP-based BCI. To this end, we firstly assessed the relevance of high frequencies (up to 60 Hz). In a second experiment we looked into the reduction of RVS amplitude depth across both low and high frequencies. Based on the results of the two previous experiments, we devised a third experiment testing different approaches for the design of comfortable stimuli with an online T9 implementation. The evaluation of an SSVEP-based BCI is usually limited to metrics such as the SNR ratio and/or classification performance. Here we propose to take an user-oriented perspective that considers visual comfort and other aspects of user experience as additional measures to evaluate the validity and usability of a reactive SSVEP-based BCI.

The first experiment disclosed that high frequencies RVS (up to 60Hz) displayed on a computer monitor could elicit measurable SSVEP responses using the RESS spatial filtering method<sup>24</sup>. These results are in line with findings from previous studies<sup>11,26</sup>. These previous studies used LEDs for the stimulation presentation which typically produce more luminosity compared to our computer screen. We used a computer screen as it offers higher flexibility for the design of reactive BCI. Solely in regards of the user-focused approach, high frequencies SSVEP appeared to be the most comfortable stimuli. Moreover, they are more likely to reduce the risks of epileptic seizure and therefore are theoretically a good idea. However, in practice the classification performances (only 54% on average for the online T9) are not substantial enough. This downgrading of performance can be seen as consequence of the 1/f trend for the magnitude of brain responses demonstrated in<sup>11</sup>. It should also be noted that the inter-subjects variability is large. Three subjects out of six have achieved satisfactory results ( $> 78\%$ ) and the three others are below 50%. Another limitation of high frequencies stimuli is that they are less perceptible and called for more focus and concentration. In brief, we have been able to decode elicited brain responses from high frequencies ( $> 30$  Hz), as previous studies, but this was not sufficient for a reliable control of the online BCI. In<sup>27</sup>, the authors have designed a neural network to decode the pattern of visual stimulation. This decoding is used in a second step to control a BCI. They have reported high variability between subjects in decoding performance for the first step, while the inter-individual differences for the control of the BCI were way lower. Thus, the capacity of decoding brain signal does not automatically and directly translate into powerful BCI control availability. On another note, high frequency SSVEP could be relevant to improve the visual comfort for basic SSVEP-based psycho-physics experiments, where usually multiple trials are averaged for post-hoc analysis and do not require single trial classification.

Our second and third experiment disclosed that the reduction of amplitude depth offers the best compromise in terms of classification performance and user experience (see Fig. 6a), as long as low frequency are considered. Importantly we report that a substantial reduction of amplitude depth, up to 50%, did not lead to a significant decrease of classification performance while improving the user comfort. Therefore it should become a standard and always consider. It should be noted that the use of high frequencies stimuli require the use of specific hardware, screens with high refresh rate while the amplitude depth reduction does not imply a more complex implementation or changes in the hardware. A larger reduction of stimulation amplitude depth could also be considered when visual comfort and fatigue become crucial, for example when the operating time is long. However, it would be at the expense of a small decrease in classification performance.

On another note, the classification speed, through Information Transfer Rate (ITR) classically mainly, is emphasized metrics to evaluate BCIs performance. The computation of the ITR takes into account the number of targets  $N$ , the classification accuracy  $P$ , the total number of trials  $S$  and  $T$  the length of the experience. In our case, the BCI provides an ITR of 38.6bpm on average for the control condition which can be low in comparison to recent studies<sup>25</sup>. One reason, is that our design includes an inter-trial of 2.5 s to allow the subject to check the output of last step and acknowledge the next figure to type. We could have asked our participant to memorize the four digits to type or have them cued and removed the classification feedback to have a reduced inter-trial of 0.2 s. It would not have impacted the classification accuracy and provided an increased ITR of 76.7 bpm which compares favorably to a benchmark study<sup>28</sup>. However, the user experience would have been drastically different with less sense of control. This shows a clear limit of the metric. As discussed in<sup>27</sup>, a trial duration (stimuli plus pause between trials) below 1 s makes the system too fast to be used by an untrained user. Beyond a certain performance threshold, improving the ITR would be usually at the expense of the user experience: trials too short for good control, increased number of errors, absence or limited feedback, etc.. These considerations about the

limitations of BCI performance measures<sup>29</sup>, especially ITR, advocate in favor of considering a trade-off between classification performance and user experience to evaluate the general performance of a BCI.

In the presented experiments, visual comfort, fatigue and frustration was assessed through self-reported questionnaires. This subjective approach allows for a direct quantification of user experience with minimal cost time and effort wise. While this approach is practical for the systematic evaluation of user experience over a wide range of stimuli, as reported here, self-report questionnaires are however subject to biases. It can therefore be argued that the acquisition of objective measures would be desirable to further validate and strengthen the present findings. As such, eye-tracking and pupillometry metrics offer valuable insights on the visual comfort and fatigue experienced by the user. Future works focusing on human factors and user experience of VEP-based BCI would benefit from including such objective measures.

To conclude, our study disclosed that the reduction of amplitude depth presented the best compromise in terms of user comfort, frustration and classification score compared to using high frequency SSVEP. We hope that this work will foster research efforts to study the effect of other stimuli features. Checkerboards have been considered<sup>30,31</sup> to increase the elicited brain response<sup>32</sup>. But in the perspective of an SSVEP-BCI, they have never been studied systematically along other textures. Instead of flickering, spatial oscillations of the flickers could also be evaluated. Beside that and still to provide better ergonomic for SSVEP-BCI system, it could be beneficial to have a gating process, such using an eye-tracker or a physical button, to make the stimuli flicker only when the user intend to interact with it. In a realistic use case, a continuous flickering would be tiring and even distracting when operating other tasks. Eventually, another bottleneck of the large use of SSVEP-BCI outside our laboratories is the hardware. In this study, we have relied on a classical wet-EEG setup. It remains tedious to equip the subject and subject should wash his air after the use. Existing hardware of dry-EEG still induce drop of accuracy compared to wet-EEG<sup>33</sup> and the comfort is not optimal<sup>34</sup>. Nevertheless, it is an important and promising approach to improve the user experience of SSVEP BCI.

## Methods

**Participants.** A total of thirty subjects took part in the study. For the first experiment focusing on the exploration of RVS frequency, 12 participants were recruited (mean age = 26, SD = 6, 8 male and 4 female). The second experiment investigating reduction of amplitude depth was performed by 12 participants (mean age = 27, SD = 5, 8 male and 4 female). The online T9 digicode BCI was tested on 6 individuals (mean age = 2, 8 SD = 4, 5 male and 1 female). The participants did not report any of the exclusion criteria (neurological antecedents, usage of psychoactive medication). The study was approved by the ethics committee of the University of Toulouse (CER approval number 2020-334) and was carried in accordance with the declaration of Helsinki. Participants gave informed written consent prior to the experiments.

**Stimuli and procedure.** One of the main challenge of SSVEP-based BCI paradigms relates to achieving precise and reliable presentation of RVS. This is especially true for the elicitation of high frequency SSVEP responses. Due to the Nyquist-Shannon sampling theorem, the highest frequency that can be presented is equal to half of the monitor maximal refresh rate. For this reason, most studies that have reported SSVEP responses above 20 Hz have used LEDs as SSVEP generator method. LED arrays as a SSVEP generator offer less flexibility for the design of comfortable RVS. Indeed, any modification of features (e.g., position, colour, size) of the LED array implies hardware replacement to be performed manually. The emergence of high frequency monitors (144 and 240 Hz) contributed to drastically extend the range of frequency that can be reliably displayed on computer monitors. Capitalizing on this technical advance, we were able to readily manipulate features of visual stimuli presented at high frequency on a computer monitor.

The stimulus presentation program was written in C for the two first experiments and in Python using Psychopy2<sup>35</sup> for the online T9 experiment. A lower-level programming language, C was preferred for the first experiment as it allowed a faster computation for the presentation of stimuli at high frequencies (above 50 Hz). This was not required for the online experiment as the frequencies selected only went up to 35 Hz. The code used for the online classification is written in Python. The Python code of the T9 graphical interface and the classification is available online ([https://github.com/ludovicdmt/t9\\_ssvep](https://github.com/ludovicdmt/t9_ssvep)). Classification was performed on EEG data and marker streams received through LSL<sup>36</sup> from the stimulus presentation program. The stimuli were presented using a sampled sinusoidal on a 27-inch LCD monitor (1ms IPS display, NVIDIA G-sync compatible), a resolution of 1920 × 1080 pixel (width × height) and a luminance of 400 cd m<sup>-2</sup>. The refresh rate was set to 240 Hz to present high frequencies with high precision. For the two first experiments stimuli were rendered within a 213 × 213 pixels rectangle centered on the screen. For the T9 experiment, each square was of size 150 × 150, with a margin of 250 pixels between each square. For the first two experiments, RVS stimuli were presented on top of a grey background whose luminance was of 124 lux (measured using a digital light meter from Extech Instruments). For the online BCI implementation, the dark background used had a luminance of 60 lux.

*Experiment 1: high against low frequencies with full amplitude of simulation.* In this first experiment we investigated the subjective experience and SSVEP in response to stimuli of a wide range of frequencies. The subjects underwent a single session that was cut in two separated parts. Firstly, we have presented sequentially and individually stimuli with twelve, low, frequencies from 8 to 30 Hz with a range of 2 Hz and then another 12, high, frequencies from 32 to 60 with a 2 Hz range (48, 50, 52 Hz were excluded because of power line noise). Half of the subjects started the session with low frequencies and the other half with high ones. Each session started with the presentation of individual flickers, low and high frequencies, alone and with a pseudo-random order, so as to fill the subjective assessment questionnaire of visual comfort and the fusion flicker frequency. Participants were asked to grade each stimulation with a mark from 1 (uncomfortable) to 10 (comfortable). We also have

presented flickers above 60Hz and asked the volunteers to acknowledge when they do not perceive the flickering anymore (fusion flicker effect). After this qualitative assessment phase, for both high and low frequencies, there were 15 blocks with one trial per class to quantitatively study the flickers. The presentation order of the frequencies inside each block was pseudo-random. Each stimulation was preceded by a red circling, visual cue, for 0.5 s, it then lasted for 3 s, followed by an inter-trial of 0.5 s. The 3 s epochs were then cut offline to accommodate for different trials lengths during analysis. Between each block there was a pause screen and subject had to press space bar when he was ready for the next block. A graphical summary of the experimental protocol and trial course can be found in Fig. 7. The total length for one session, including the setup of the wet-EEG and the questionnaire, was less than one hour. As in this currently the state of the art classifier for synchronous SSVEP, we have used Task Related Component Analysis (TRCA)<sup>25</sup> as classifier in the offline analysis. Further details on the classifier are provided in the following methods sections (page 11) and in the Supplementary Information. For both high and low frequencies condition, the background was set to gray and flickers oscillated between gray and white. Twelve healthy individuals (4 female, mean age = 26, SD = 6 SD) took part in the single session of this experiment.

*Experiment 2: reducing amplitude depth of simulation.* In the second experiment, our aim was to explore a reduction in the amplitude depth of stimulation for both high and low frequencies stimuli. We have quantitatively and qualitatively studied the trade-off between accuracy and user comfort for reduced amplitude stimuli. To the best of authors knowledge, while the use of a broader range of frequencies was studied, mostly with LED, a reduction of stimulation amplitude to control a BCI was only consider in a preliminary quantitative study<sup>22</sup>. Consistent with the conclusions of the Experiment 1, we have selected 12, 14, 16 and 18 Hz as for the low frequencies condition and 32, 34, 36 and 38 Hz for the high frequencies. The number of trials and stimulus presentation duration was kept consistent with Experiment 1: 15 trials, 0.5 s of cue, 3 s stimulation and inter trial of 0.5 s with a self-paced break (space bar press to continue) between blocks. Prior to the experiment, the perceptual threshold for the minimal amplitude depth was assessed through a staircase procedure (starting from 5% of the maximal amplitude depth with decrements of 0.1%). Then the session started with the subjective assessment of each flicker with the different amplitude depths, before switching to the blocks presentation and EEG recording. The amplitude depth was manipulated across six levels (100%, 80%, 60%, 50%, 40%, 30%). The definition of the range was so to achieve good sensitivity from 30 up to 100%, with lowest amplitude depths being doubled (30, 40 and 50 with the corresponding 60, 80 and 100%). The total duration of Experiment 2 was twice as long as Experiment 1. It was therefore split in two sessions to avoid fatigue effects. The order of conditions was also counterbalanced across participants. The two sessions took place on different days and were separated by a maximum of 1 week. The experimental protocol and trial course are depicted in Fig. 7.

In practice the implementation of the amplitude depth reduction used a sinusoidal sampled to the refresh rate of the screen. The background was set to gray as in Experiment 1. The RVS were oscillating from gray (value of 130 on the gray scale) to white (value of 255 on the gray scale) for full amplitude and from gray to lighter shades of gray for the amplitude depth reduction RVS. For instance, a RVS with reduced amplitude of 40% would oscillate between  $130 + (255 - 130) \times 0.4 = 180$  on the gray scale. The maximum depth reduction that allows perception of RVS contrast change was also an open question which was investigated in Experiment 2. The rationale for and the definition of this perceptual threshold is comparable to the fusion-flicker threshold procedure described in Experiment 1. We used TRCA as in Experiment 1 for the offline classification analysis. Twelve healthy individuals (4 female, mean age = 27, SD = 5.25) took part in both sessions of this experiment. Four participants had already taken part to the first experiment.

*Experiment 3: an online T9 experiment with improved visual comfort.* This third experiment was designed to test the validity of high frequency and low amplitude stimuli in the context of a realistic SSVEP-based BCI. Based on the previous findings from experiments 1 and 2, we formulated the hypothesis that high frequency and low amplitude RVS can improve user experience while maintaining high classification performances for BCI control. This study also aimed to investigate the limitations of high frequency stimuli in an online BCI context. The classification was therefore performed online and direct feedback was provided to the user.

The BCI consists of a T9 keyboard, smartphone keyboard, with numbers from 0 to 9, and *Back* (11 classes problem). We have asked the participants to type 10 codes of 4 numbers, PIN codes. The specified PIN code was displayed on the left of the T9 and the output of the BCI on the left. You can find a screen-shot of the interface in the Supplementary Information. In addition to the visual feedback on the right of the screen, an auditory feedback was provided with a low-pitch tone for an error of classification and a high-pitch tone for a correct classification. Background color was set to black to further improve contrast with the RVS.

The following three conditions were tested. High frequencies (30–34.6 Hz) and slightly reduced amplitude (90%) stimuli [HF]. Low frequencies (10–14.6 Hz) and largely reduced amplitude depth (50%) [LF-LA]. And Low frequencies (10–14.6 Hz) with full amplitude depth [LF-HA] as a control condition reflecting the classical RVS design used in previous SSVEP-based BCI.

To display the 11 classes within a reduced frequency range of 4.6 Hz, we took advantage of the Joint Frequency and Phase Modulation (JFPM)<sup>37</sup>, as used in the original paper of the state of the art method TRCA<sup>25</sup>. The RVS frequency were vertically spaced of 0.2 Hz with phases differences of  $+0.35\pi$  and horizontally spaced with 2 Hz with phases differences of  $-0.5\pi$ , using sine waves. This implementation is schematized in the Supplementary Information. The RVS were oscillating between black and white. Similarly to previous experiments, we have used the TRCA classifier<sup>25</sup>. Trial length was set to 2.0s to maximize accuracy over ITR, as discussed on 7. In order to ensure a reliable classification accuracy, 12 calibration samples were collected for each class. This approach is comparable to the original TRCA study<sup>25</sup> that used 10 calibration sample per class. The calibration

was divided in 12 blocks, within which each class was presented as a target once. The presentation order was pseudo-randomized and different for each block. One of the stimulus was cued for 0.5 s with a red circling. Then, the stimulation lasted for 2.13 s and only the last 2.0 s were kept. The first 0.13 s of the stimulation period were discarded to account for a latency delay of information going through the visual pathway<sup>38</sup>. Finally, a pause of 0.7 s as inter-trial was completed. During the online test phase, the inter-trial was set to 2.5 s to allow the user to check between each trial the specified PIN code on the left and output from previous commands on the right. We could have reduced the inter-trial time to increase the ITR but our aim was to have a user-friendly interface that allows realistic interactions with the BCI. Stimulation was also set to 2s during the test phase. The pause duration between calibration blocks and the input of 4 consecutive digits PIN code was left to participants' appreciation (space bar had to be pressed to continue the experiment). Six healthy individuals (1 female, 7 males, mean age = 28, SD = 4) took part in the single session of this experiment.

**EEG data acquisition.** EEG data was recorded from 32 electrodes fitted in an elastic cap according to the 10–20 international system and connected to a LiveAmp amplifier (Brain Products, Munich, Germany). The ground electrode was placed at the Fpz electrode location and all electrodes were referenced to FCz electrode. The electrode impedance were brought below  $20k\Omega$  prior recording. The signal was acquired at a rate of 500 Hz with a digital band-pass filter ranging from 0.1 to 250 Hz. At the onset of every stimulus presentation, an event trigger was generated by the stimulus presentation program and synchronized to the EEG data stream via Lab Streaming Layer (LSL)<sup>36</sup>. Eventually, only height electrodes (O1, O2, Oz, P3, P4, Pz, P7, P8) are manually selected to perform classification while all electrodes are used for Fourier frequency analyses. The manual selection of electrodes was centered around the occipital region. The raw data from the three experiments, with all electrodes included, are available online <https://zenodo.org/record/5907009>.

**Subjective tests.** In each experiment, questionnaires assessing participants' subjective experience of RVS were administered to gather information about how visually comfortable, tiring and intrusive the stimuli were deemed. For this, RVS were presented for three seconds to the participants. Then the participants rated the RVS in terms of the three aforementioned dimensions (visual comfort, fatigue, intrusiveness) by assessing them on analog scales ranging from 1 to 10. This procedure was repeated for each condition of the corresponding experimental design. The presentation order of the RVS within these subjective assessment trials was randomized across participants.

**SSVEP analysis.** Rhythmic Entrainment Source Separation (RESS) algorithm<sup>24</sup> is a supervised source separation technique. It was used to assess in an offline manner the signal quality and characteristics from the Experiment 1 and 2. It computes a spatial filter  $w$  that is intended to extract the signal of interest elicited by the SSVEP. The filter  $w$  maximizes the covariance matrix of data filtered, narrowly, around the SSVEP frequency of interest while minimizing covariance matrix out of the narrow band. The SSVEP activity is supposed spatially stationary over time and thus  $w$  is computed only one time for all trials.

**Classification algorithm.** We have selected Task-Related Component Analysis (TRCA)<sup>25</sup> algorithm that is state of the art for SSVEP to assess classification performance with regards to the different stimuli designs. TRCA model achieved more than 90% accuracy and Information Transfer Rate (ITR) of more than 300 bits/min on a 40 classes Brain Speller, using 0.5s epochs. It has been since largely endorsed by the community, even using dry electrodes<sup>33</sup>. The other classical classification algorithms for SSVEP are based on Canonical Correlation Analysis (CCA)<sup>39,40</sup>, with multiple nuances to define EEG template to compare with. In<sup>25</sup>, these CCA-based methods provided significantly lower results compared to TRCA. Therefore, we chose to compute results only with the TRCA method. It would represent classical, generic and state of the art framework for SSVEP classification. Beside that, some incremental gains of performance could be provided by more calibration data but it would not have been in favor of a better user experience. More details on the TRCA algorithm can be found in the Supplementary Information. In our study, we observed better results when applying a downsampling of factor 2 to have a sampling rate of 250Hz, as is the original paper of TRCA. We used a Python implementation by our team (<https://github.com/nbara/python-meegkit/blob/master/meegkit/trca.py>), based on the original Matlab code shared by the authors, that can be found here (<https://github.com/mnakanishi/TRCA-SSVEP>).

## Data availability

The datasets generated and analysed during the current study are available in the Zenodo repository, <https://zenodo.org/record/5907009>.

Received: 17 February 2022; Accepted: 9 May 2022

Published online: 25 May 2022

## References

- Wu, Z., Lai, Y., Xia, Y., Wu, D. & Yao, D. Stimulator selection in SSVEP-based BCI. *Med. Eng. Phys.* **30**, 1079–1088 (2008).
- Joon Kim, Y., Graboweczyk, M., Paller, K. A., Muthu, K. & Suzuki, S. Attention induces synchronization-based response gain in steady-state visual evoked potentials. *Nat. Neurosci.* **10**, 117–125 (2007).
- Zhu, D., Bieger, J., Garcia Molina, G. & Aarts, R.M. A survey of stimulation methods used in SSVEP-based BCIs. *Comput. Intell. Neurosci.* **2010** (2010).
- Zemon, V. M. & Gordon, J. Luminance-contrast mechanisms in humans: Visual evoked potentials and a nonlinear model. *Vis. Res.* **46**, 4163–4180 (2006).

5. Duszyk, A. *et al.* Towards an optimization of stimulus parameters for brain-computer interfaces based on steady state visual evoked potentials. *PLoS ONE* **9**, 1–11 (2014).
6. Wu, C.-H. & Lakany, H. The effect of the viewing distance of stimulus on SSVEP response for use in brain-computer interfaces. in *Proceedings 2013 IEEE International Conference on Systems, Man and Cybernetics (SMC)*. 1840–1845. (2013).
7. Patterson Gentile, C. & Aguirre, G. K. A neural correlate of visual discomfort from flicker. *J. Vis.* **20**, 11 (2020).
8. Pastor, M. A., Artieda, J., Arbizu, J., Valencia, M. & Masdeu, J. C. Human cerebral activation during steady-state visual-evoked responses. *J. Neurosci.* **23**, 11621–11627 (2003).
9. Ng, K. B., Bradley, A. P. & Cunnington, R. Stimulus specificity of a steady-state visual-evoked potential-based brain-computer interface. *J. Neural Eng.* **9** (2012).
10. Fisher, R. S., Harding, G., Erba, G., Barkley, G. L. & Wilkins, A. Photic- and pattern-induced seizures: A review for the epilepsy foundation of America Working Group (2005).
11. Herrmann, C. S. Human EEG responses to 1–100 Hz flicker: Resonance phenomena in visual cortex and their potential correlation to cognitive phenomena. *Exp. Brain Res.* **137**, 346–353 (2001).
12. Diez, P. F., Mut, V. A., Avila Perona, E. M. & Laciár Leber, E. Asynchronous BCI control using high-frequency SSVEP. *J. NeuroEng. Rehabil.* **8**, 39 (2011).
13. Müller, S. M. T. *et al.* SSVEP-BCI implementation for 37–40 Hz frequency range. *Proc. Annu. Int. Conf. IEEE Eng. Med. Biol. Soc. EMBS* **1**, 6352–6355 (2011).
14. Chabuda, A., Durka, P. & Zygierewicz, J. *High frequency SSVEP-BCI with hardware stimuli control and phase-synchronized comb filter* (IEEE Transactions on Neural System Rehabilitation Engineering, 2018).
15. Ajami, S., Mahnam, A. & Abootalebi, V. Development of a practical high frequency brain-computer interface based on steady-state visual evoked potentials using a single channel of EEG. *Biocybern. Biomed. Eng.* **38**, 106–114 (2018).
16. Liang, L., Yang, C., Wang, Y. & Gao, X. High-frequency SSVEP stimulation paradigm based on dual frequency modulation?. *Proc. Annu. Int. Conf. IEEE Eng. Med. Biol. Soc. EMBS*, 6184–6187. (2019).
17. Yue, L. *et al.* A brain-computer interface based on high-frequency steady-state asymmetric visual evoked potentials. in *2020 42nd Annual International Conference of the IEEE Engineering in Medicine Biology Society (EMBC)*. 3090–3093. (2020).
18. Wandell, B. A., Dumoulin, S. O. & Brewer, A. A. Visual field maps in human cortex. (2007).
19. Baseler, H. A., Sutter, E. E., Klein, S. A. & Carney, T. The topography of visual evoked response properties across the visual field. *Electroencephalogr. Clin. Neurophysiol.* **90**, 65–81 (1994).
20. Chang, M. H., Baek, H. J., Lee, S. M. & Park, K. S. An amplitude-modulated visual stimulation for reducing eye fatigue in SSVEP-based brain-computer interfaces. *Clin. Neurophysiol.* **125**, 1380–1391 (2014).
21. Lingelbach, K. *et al.* Brain oscillation entrainment by perceptible and non-perceptible rhythmic light stimulation. *Front. Neuroergonomics* **2** (2021).
22. Ladouce, S., Torre Tresols, J. J., Darmet, L., Ferraro, G. & Dehais, F. Improving user experience of SSVEP-BCI through reduction of stimuli amplitude depth. in *(IEEE 2021)* (IEEE, 2021).
23. Eisen-Enosh, A., Farah, N., Burgansky-Eliash, Z., Polat, U. & Mandel, Y. Evaluation of critical flicker-fusion frequency measurement methods for the investigation of visual temporal resolution. *Sci. Rep.* (2017).
24. Cohen, M. & Gulbinaite, R. Rhythmic entrainment source separation: Optimizing analyses of neural responses to rhythmic sensory stimulation. *NeuroImage* **147**, 43 (2016).
25. Nakanishi, M. *et al.* Enhancing detection of SSVEPs for a high-speed brain speller using task-related component analysis. *IEEE Trans. Biomed. Eng.* **65**, 104–112 (2018).
26. Sakurada, T., Kawase, T., Komatsu, T. & Kansaku, K. Use of high-frequency visual stimuli above the critical flicker frequency in a SSVEP-based BMI. *Clin. Neurophysiol.* **126**, 1972–1978 (2015).
27. Nagel, S. & Spüler, M. World's fastest brain-computer interface: Combining EEG2Code with deep learning. *PLOS ONE* **14**, 1–15 (2019).
28. Nakanishi, M., Wang, Y., Wang, Y.-T. & Jung, T.-P. A comparison study of canonical correlation analysis based methods for detecting steady-state visual evoked potentials. *PLoS one* **10**, e0140703 (2015).
29. Yuan, P. *et al.* A study of the existing problems of estimating the information transfer rate in online brain-computer interfaces. *J. Neural Eng.* (2013).
30. Funase, A., Wakita, K., Itai, A. & Takumi, I. SSVEP by checkerboard related to grid size and board size. in *2015 Asia-Pacific Signal and Information Processing Association Annual Summit and Conference (APSIPA)*. 1141–1144. (2015).
31. Waytowich, N. R., Yamani, Y. & Krusinski, D. J. Optimization of checkerboard spatial frequencies for steady-state visual evoked potential brain computer interfaces. *IEEE Trans. Neural Syst. Rehabil. Eng.* **25**, 557–565 (2017).
32. Reynolds, J. H., Pasternak, T. & Desimone, R. Attention increases sensitivity of V4 neurons. *Neuron* **26**, 703–714 (2000).
33. Xing, X. *et al.* A high-speed SSVEP-based BCI using dry EEG electrodes. *Sci. Rep.* **8** (2018).
34. Oliveira, A. S., Schlink, B. R., Hairston, W. D., König, P. & Ferris, D. P. Proposing metrics for benchmarking novel EEG technologies towards real-world measurements. *Front. Hum. Neurosci.* **10**, 188 (2016).
35. Peirce, J. *et al.* PsychoPy2: Experiments in behavior made easy. *Behav. Res. Methods* **51** (2019).
36. Kothe, C., Medine, D., Boulay, C., Grivich, M. & Stenner, T. Lab streaming layer. <https://github.com/sccn/labstreaminglayer> (2014).
37. Chen, X. *et al.* High-speed spelling with a noninvasive brain-computer interface. in *Proceedings of the National Academy of Sciences of the United States of America*. Vol. 112. (2015).
38. Lee, J., Birtles, D., Wattam-Bell, J., Atkinson, J. & Braddick, O. Latency measures of pattern-reversal VEP in adults and infants: Different information from transient P1 response and steady-state phase. *Investig. Ophthalmol. Vis. Sci.*<https://doi.org/10.1167/iovs.11-7631> (2012).
39. Nakanishi, M., Wang, Y., Wang, Y.-T., Mitsukura, Y. & Jung, T.-P. A high-speed brain speller using steady-state visual evoked potentials. *Int. J. Neural Syst.* **24**, 1450019 (2014).
40. Wang, Y., Nakanishi, M., Wang, Y.-T. & Jung, T.-P. Enhancing detection of steady-state visual evoked potentials using individual training data. in *2014 36th Annual International Conference of the IEEE Engineering in Medicine Biology Society EMBC 2014*. Vol. 2014. (2014).

## Acknowledgements

This research was funded by the *Agence Innovation Défense* of the *Direction Générale de l'Armement*. The authors would also like to acknowledge the Artificial and Natural Intelligence Toulouse Institute (ANITI) and the Axa Research fund Neuroergonomics chair for flight safety for currently funding our team.

## Author contributions

S.L., L.D., J.J.T.T., G.F. and F.D. designed the experiment. J.J.T.T., S.V. and L.D. coded the stimulus presentation program. S.L. collected the data. S.L. and L.D. performed analyses. S.L., L.D. and F.D. wrote the manuscript.

### Competing interests

The authors declare no competing interests.

### Additional information

**Supplementary Information** The online version contains supplementary material available at <https://doi.org/10.1038/s41598-022-12733-0>.

**Correspondence** and requests for materials should be addressed to S.L.

**Reprints and permissions information** is available at [www.nature.com/reprints](http://www.nature.com/reprints).

**Publisher's note** Springer Nature remains neutral with regard to jurisdictional claims in published maps and institutional affiliations.



**Open Access** This article is licensed under a Creative Commons Attribution 4.0 International License, which permits use, sharing, adaptation, distribution and reproduction in any medium or format, as long as you give appropriate credit to the original author(s) and the source, provide a link to the Creative Commons licence, and indicate if changes were made. The images or other third party material in this article are included in the article's Creative Commons licence, unless indicated otherwise in a credit line to the material. If material is not included in the article's Creative Commons licence and your intended use is not permitted by statutory regulation or exceeds the permitted use, you will need to obtain permission directly from the copyright holder. To view a copy of this licence, visit <http://creativecommons.org/licenses/by/4.0/>.

© The Author(s) 2022

## Terms and Conditions

Springer Nature journal content, brought to you courtesy of Springer Nature Customer Service Center GmbH (“Springer Nature”).

Springer Nature supports a reasonable amount of sharing of research papers by authors, subscribers and authorised users (“Users”), for small-scale personal, non-commercial use provided that all copyright, trade and service marks and other proprietary notices are maintained. By accessing, sharing, receiving or otherwise using the Springer Nature journal content you agree to these terms of use (“Terms”). For these purposes, Springer Nature considers academic use (by researchers and students) to be non-commercial.

These Terms are supplementary and will apply in addition to any applicable website terms and conditions, a relevant site licence or a personal subscription. These Terms will prevail over any conflict or ambiguity with regards to the relevant terms, a site licence or a personal subscription (to the extent of the conflict or ambiguity only). For Creative Commons-licensed articles, the terms of the Creative Commons license used will apply.

We collect and use personal data to provide access to the Springer Nature journal content. We may also use these personal data internally within ResearchGate and Springer Nature and as agreed share it, in an anonymised way, for purposes of tracking, analysis and reporting. We will not otherwise disclose your personal data outside the ResearchGate or the Springer Nature group of companies unless we have your permission as detailed in the Privacy Policy.

While Users may use the Springer Nature journal content for small scale, personal non-commercial use, it is important to note that Users may not:

1. use such content for the purpose of providing other users with access on a regular or large scale basis or as a means to circumvent access control;
2. use such content where to do so would be considered a criminal or statutory offence in any jurisdiction, or gives rise to civil liability, or is otherwise unlawful;
3. falsely or misleadingly imply or suggest endorsement, approval , sponsorship, or association unless explicitly agreed to by Springer Nature in writing;
4. use bots or other automated methods to access the content or redirect messages
5. override any security feature or exclusionary protocol; or
6. share the content in order to create substitute for Springer Nature products or services or a systematic database of Springer Nature journal content.

In line with the restriction against commercial use, Springer Nature does not permit the creation of a product or service that creates revenue, royalties, rent or income from our content or its inclusion as part of a paid for service or for other commercial gain. Springer Nature journal content cannot be used for inter-library loans and librarians may not upload Springer Nature journal content on a large scale into their, or any other, institutional repository.

These terms of use are reviewed regularly and may be amended at any time. Springer Nature is not obligated to publish any information or content on this website and may remove it or features or functionality at our sole discretion, at any time with or without notice. Springer Nature may revoke this licence to you at any time and remove access to any copies of the Springer Nature journal content which have been saved.

To the fullest extent permitted by law, Springer Nature makes no warranties, representations or guarantees to Users, either express or implied with respect to the Springer nature journal content and all parties disclaim and waive any implied warranties or warranties imposed by law, including merchantability or fitness for any particular purpose.

Please note that these rights do not automatically extend to content, data or other material published by Springer Nature that may be licensed from third parties.

If you would like to use or distribute our Springer Nature journal content to a wider audience or on a regular basis or in any other manner not expressly permitted by these Terms, please contact Springer Nature at

[onlineservice@springernature.com](mailto:onlineservice@springernature.com)